THE EFFICIENCY IMPROVEMENT PROGRAM FOR THE WJ-274 TRAVELING-WAVE TUBE

By Lester A. Roberts

Prepared under Contract No. NAS1-5923 by

WATKINS-JOHNSON COMPANY
Palo Alto, California

for

NATIONAL AERONAUTICS AND SPACE ADMINISTRATION
LANGLEY RESEARCH CENTER

THE EFFICIENCY IMPROVEMENT PROGRAM FOR THE WJ-274 TRAVELING-WAVE TUBE

By Lester A. Roberts
The Watkins-Johnson Company
Palo Alto, California

SUMMARY

This report describes the work done for the NASA, Langley Research Center on the WJ-274, a 20 watt space-type traveling-wave tube. The purpose of the program is to study techniques to further improve its overall efficiency characteristics.

The studies resulted in the development of a single helix, PPM focused traveling-wave tube capable of delivering 25 watts of power output at 2.3 GHz at an overall efficiency (including heater) of 42.2 percent. These characteristics are achieved with a saturation gain of 34 dB.

TABLE OF CONTENT

LIST OF ILLUSTRATIONS

List of Illustrations (continued)

I. INTRODUCTION

This program was undertaken at Watkins-Johnson Company for the NASA Langley Research Center with the purpose of improving the efficiency performance of a small, lightweight traveling-wave tube known as the WJ-274. This tube was developed expressly for space telemetry applications on a program previously sponsored by the Langley Research Center. Versions of this tube have been space qualified and are currently being used on such programs as the Saturn V Launch Vehicle where it performs in the vital role of the principal component of the telemetry and tracking transmitters.

The original RF power output level requirements were specified as 20 watts. Subsequent use of the tube in actual space amplifier systems showed that it is necessary to operate the tube at the 23 to 25 watt power output level in order to realize a minimum out of the power amplifier system of 20 watts. This is necessary to compensate for harmonic filter and output circulator losses, slight power supply voltage changes due to the temperature environment and line voltage changes over which a practical system must operate. For 20 watt systems, the required tube power level will be considered to be 25 watts.

Background of High Efficiency Work at Watkins-Johnson

Considerable emphasis has been placed on the achievement of high efficiency in traveling-wave tubes at Watkins-Johnson Company over the last several years. This has been particularly aimed in the direction of space type tubes because of the importance of efficiency in the limited primary power budget of orbiting and deep space telemetry and communication systems.

Either preceding or concurrent with the present WJ-274 development program there have been several programs which have prime emphasis on efficiency:

The Original WJ-274 Development Program

This program, sponsored by the NASA Langley Research Center, began with the goal of achieving 20 watts of power output at 40 percent efficiency at 2.3 GHz. The concept of efficiency improvement through large overvoltage techniques was pioneered on this program. Forty percent overall efficiency was achieved at the 35 watt level and 37.8 percent efficiency was demonstrated at the 20 watt level.

The TWT Efficiency Research Program

This program, sponsored by the U. S. Army Electronics Command (USAECOM), was a basic study into the large signal characteristics and parameters of traveling-wave tubes with the emphasis on developing new techniques for obtaining high efficiency. Early in the program the spent electron beam emerging from the helix under small signal and saturation conditions was analyzed with velocity and current analyzers. Based upon the measured beam characteristics two variations of the standard traveling-wave tube configuration were devised in an effort to enhance efficiency performance. These two variations have become known as the two-helix approach and the positive taper approach. Both devices demonstrated beam efficiencies in excess of 40 percent and efficiencies with depressed collector (not including heater) of greater than 50 percent. Both of these ideas were used on the present program.

Company Sponsored High Efficiency Study Program

Because of the very promising results of the USAECOM program, Watkins-Johnson began a company-sponsored program to study the effects of variations of the various tube parameters and their related effect upon efficiency. The emphasis of this program was to obtain a basis for scaling tube designs to different power levels and frequencies. A version of the USAECOM tube was built which could be more readily adapted to scaling of PPM focused tubes. This program is continuing at the present time with the emphasis on achieving quantitative agreement between large signal digital computer calculations and measured large signal, high efficiency performance characteristics of some of the traveling-wave tubes built on the program.

The 100 Watt Development Program

This program, sponsored by the Jet Propulsion Laboratory of the California Institute of Technology, has a design goal of 100 watts output at 2.3 GHz with an efficiency goal of 55 percent. This is a PPM tube development with space type hardware as an end goal. At the present time, 45 percent efficiency has been achieved at the 100 watt level. Development is still underway.

APPENDIX II

PERFORMANCE SUMMARY OF WJ-274-1 TUBES BUILT BOTH BY R & D AND PRODUCTION

The WJ-274-1 is a tube developed for the Saturn V Instrumentation Unit (IU). After the initial development of the tube, a number of tubes were built by the R & D group for delivery. Later a production run of another group of tubes was made by the production group. The power output, gain and efficiency characteristics of these two groups of tubes are shown in Fig. II-1. It is interesting to note that both the R & D and the production runs had the same small spread in both saturation gain and overall efficiency. The average value of efficiency for both groups was 34 percent.

II. SIGNIFICANT PROGRAM ACCOMPLISHMENTS WITH SINGLE-HELIX TECHNOLOGY ON THE WJ-274

A. General Results

In general, three basic performance characteristics of the WJ-274 have been improved over the characteristics which existed at the beginning of the program.

The first and most important is the achievement of an overall efficiency (including heater) of 42.2 percent at a power level of 25.7 watts. The best previous efficiency on a WJ-274 at this power level was 37.8 percent which was achieved during the previous program.

The second important achievement was to improve the RF input-output characteristics in the vicinity of saturation. The range over which the power input could be varied for an output change of less than 0.5 dB was broadened to almost 5 dB. This makes the tube less sensitive to the power stability of the drive source and also leads to less critical requirements on the regulation capability of the power supply voltages. Incidental to this improved saturation characteristic, the small signal gain characteristic has been improved so that small signal and saturation gain differ by only 3 dB. The large change from low values of small signal gain to normal values of saturation gain which are characteristic of highly overvoltaged tubes has been eliminated.

The third important characteristic which was demonstrated showed that saturation gains of 30 to 35 dB could be achieved with no degradation of tube efficiency. Previously, the WJ-274 tubes which exhibited high values of efficiency had gain values in the range of 18 to 22 dB. The demonstration of simultaneous high gain and high efficiency now reduces the power level requirements of the RF drive source to less than 10 MW. This power requirement will considerably improve the reliability of the drive source. Furthermore, it improves the overall system efficiency by reducing the dc power input required by the typically inefficient solid state exciter.

B. Detailed Results

Experimental versions of the WJ-274 were built on this program running from serial numbers 10 through 18. The designs which achieved significant results were incorporated in tubes 13, 17, 18 and WJ-274-6 No. 2. These tubes will be discussed in detail in this section. Details of the other tubes will be covered in another section.

WJ-274 No. 13

Overall efficiency of the WJ-274 No. 13 reached a peak value of 41.7 percent at the power output level of 25 watts. Efficiency exceeds 40 percent over the output range of 20 to 30 watts. This is shown in Fig. 1 where in addition to overall effiency, beam efficiency and depressed efficiency are plotted. Beam efficiency is the basic efficiency of the device, and it is seen that overall efficiency is a maximum where beam efficiency is a maximum. Beam efficiency is the RF power output divided by the product of helix voltage and beam current. The depressed efficiency curve shows the extent to which the beam efficiency can be enhanced by collector depression. At the best power level, efficiency is raised to 43.7 percent by collector depression which is an improvement factor of 1.39. The overall efficiency value includes the power dissipation of the heater. The difference between the upper two curves decreases as the power level of operation increases because the heater power becomes a smaller fraction of the total power input to the tube.

Design

The design of tube no. 13 was scaled from the "positive taper tube" no. 1 of the USAECOM program. The term "scaled" should be qualified because not all parameters could be scaled. Fortunately, the perveance and the γa of the WJ-274 and the USAECOM tube no. 1 were close to the same values. The operating frequencies were in the ratio of 1.0 GHz to 2.3 GHz. The WJ-274 no. 13 had to be constructed within the restriction of using the same body and helix diameter as the normal WJ-274 which meant that the ratio of the bodywall diameter to mean helix diameter would not be the same as the USAECOM tube no. 1. The helix lengths were chosen to have the same values of BCN at small signal synchronism. It was felt that this should give close to the same gain under over-voltage conditions because of the similarity of the other controlling parameters of the two tubes.

The helix design of this tube is detailed in Appendix I. Note that approximately one-third of the active helix is ahead of the attenuator and two-thirds follow the attenuator. When the same TPI of the helix is used ahead and behind the attenuator, these relative lengths lead to a saturation gain under maximum efficiency conditions of approximately 20 dB. Higher gains can be obtained with input helix modifications from this configuration, but this configuration represents a reference situation from which performance variations due to design changes can be evaluated.

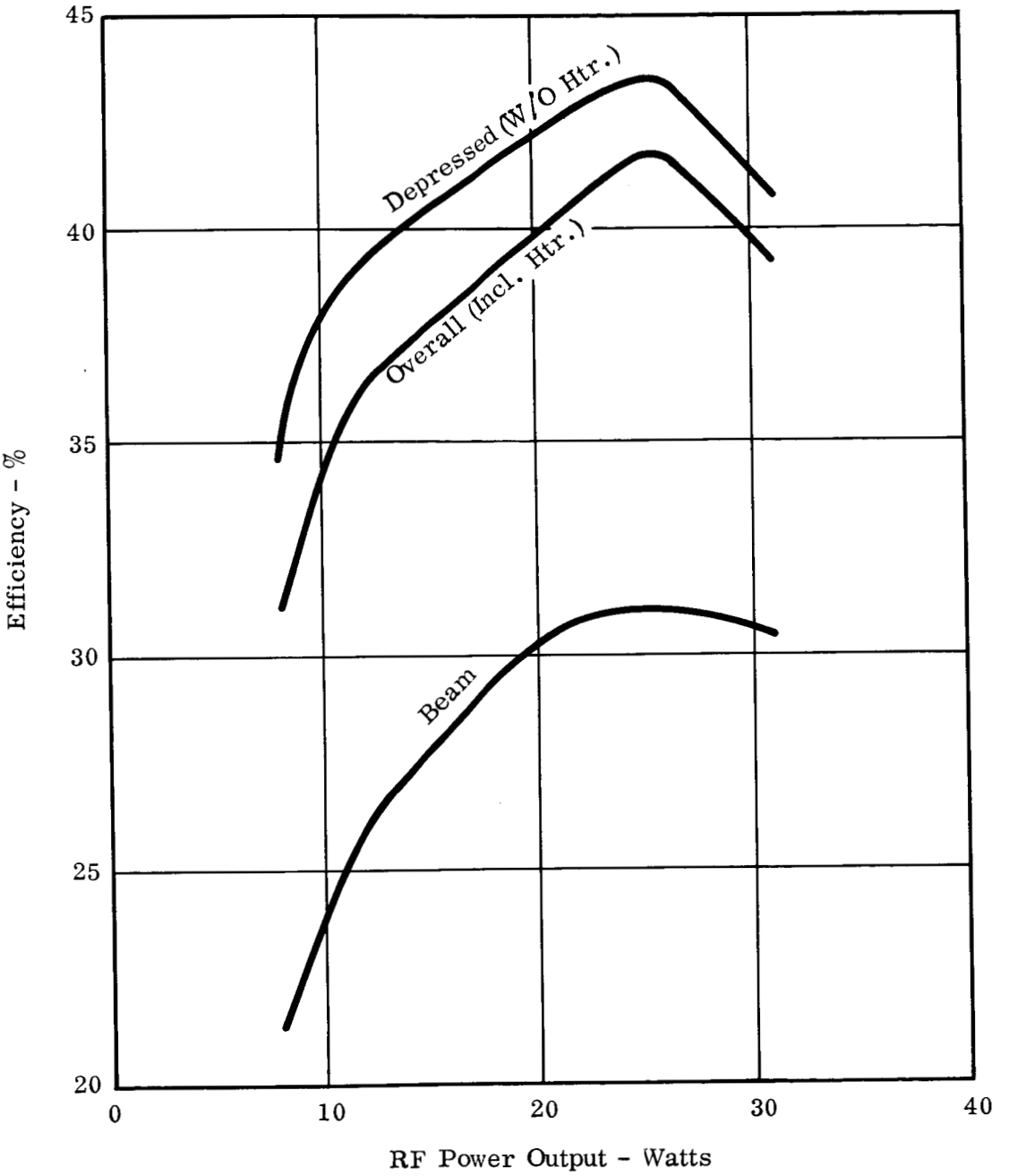

Fig. 1 - Efficiency characteristics achieved versus RF power level for WJ-274 No. 13.

17932

Figure 2 shows beam efficiency performance versus helix voltage with beam current as the parameter. To correctly understand these curves, it should be realized that each point on the curves represents a measurement under saturation power output conditions. It is seen that for a fixed value of beam current, efficiency increases with helix voltage until it reaches a maximum then decreases. At each successive increase of current, the efficiency rises to a higher value and the efficiency maximum moves to a higher helix voltage. Finally at the 45 mA condition, the efficiency reaches its highest peak. The peak values of efficiency then decrease for higher values of beam current. Note that the values of RF power output are indicated at the maximum efficiency points for the three highest curves. These lie in the desired range of 20 to 25 watts out. It should be noted that this is pre-fade data taken to show the true interaction properties of the tube without the effect of the losses due to helix and dielectric heating. Fading under continuous conditions at the highest power levels amounted to 0.2 dB or less.

Figure 3 shows the saturation gain associated with each point on the curves of Fig. 2. It is seen that the saturation gain decreases with increasing helix voltage. At the higher beam currents the gain is a linearly decreasing function of helix voltage. If the points corresponding to the peaks of the efficiency curves are plotted on the gain curves, a locus of points is found which lies between 20 and 23 dB over the entire range of helix voltage. This is shown as the dashed curve in Fig. 3. The implication of this is that the efficiency is limited by the gain beyond the attenuator. When the gain beyond the attenuator reduces to a value of about 26 dB, the large signal effects in the beam reach from the output of the helix all the way back to the attenuator.* At this point, any further decrease in gain does not allow the proper relationship to be established between the fundamental component of RF helix voltage and the fundamental component of the RF beam current and efficiency then decreases rapidly with further overvoltaging.

---

* The overall gain of the tube is less than the gain beyond the attenuator because of the 7 dB launching loss in the input helix section and the approximately 6 dB "sever loss" due to the beam drifting through the field free attenuator region and having to establish the growing wave beyond the attenuator. The net gain of the input section is insufficient to compensate for these losses and as a result the overall gain of the tube is less than the gain beyond the attenuator.

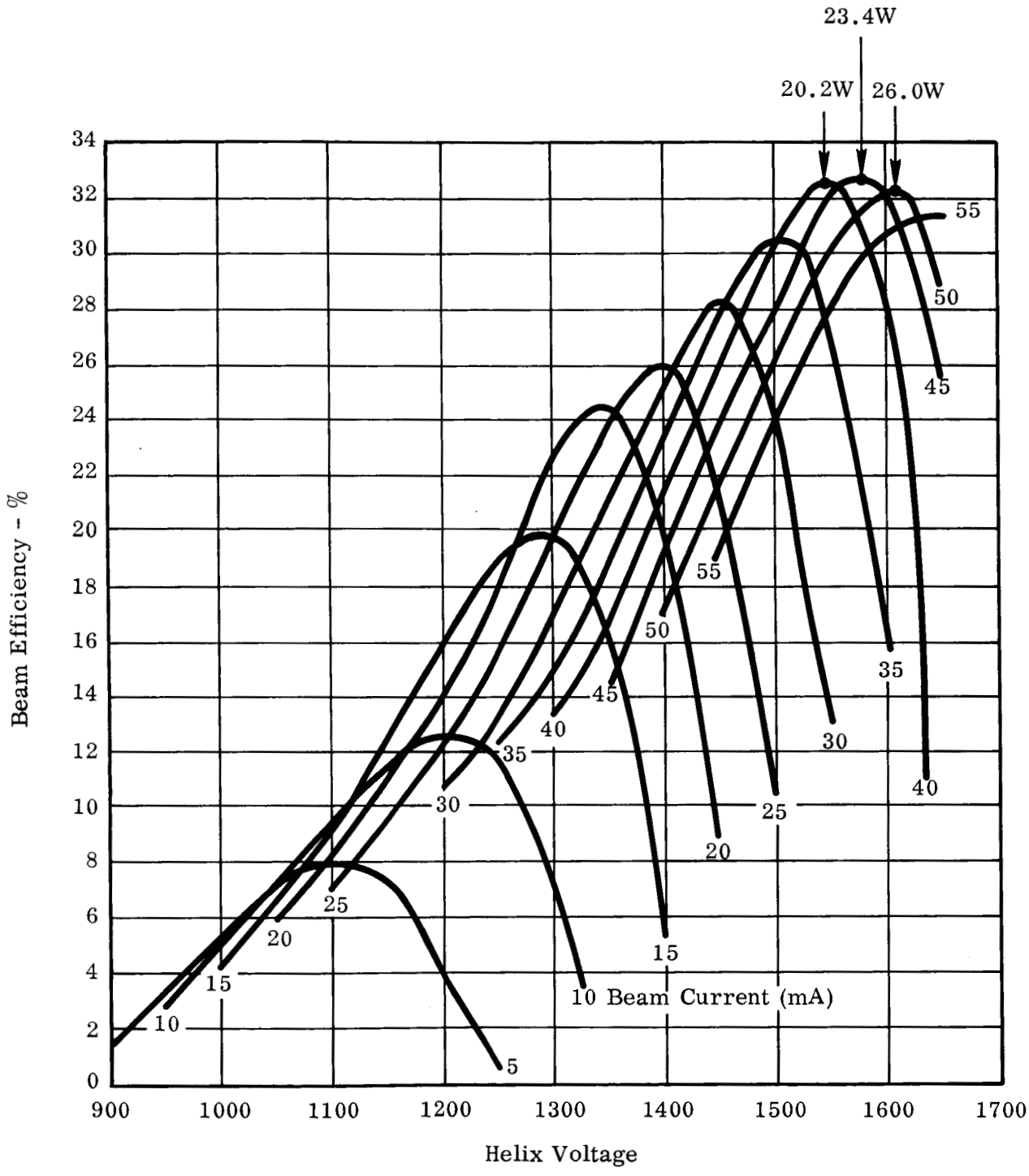

Fig. 2 - Beam efficiency versus helix voltage with beam current as the parameter for WJ-274 No. 13 at 2.3 GHz.

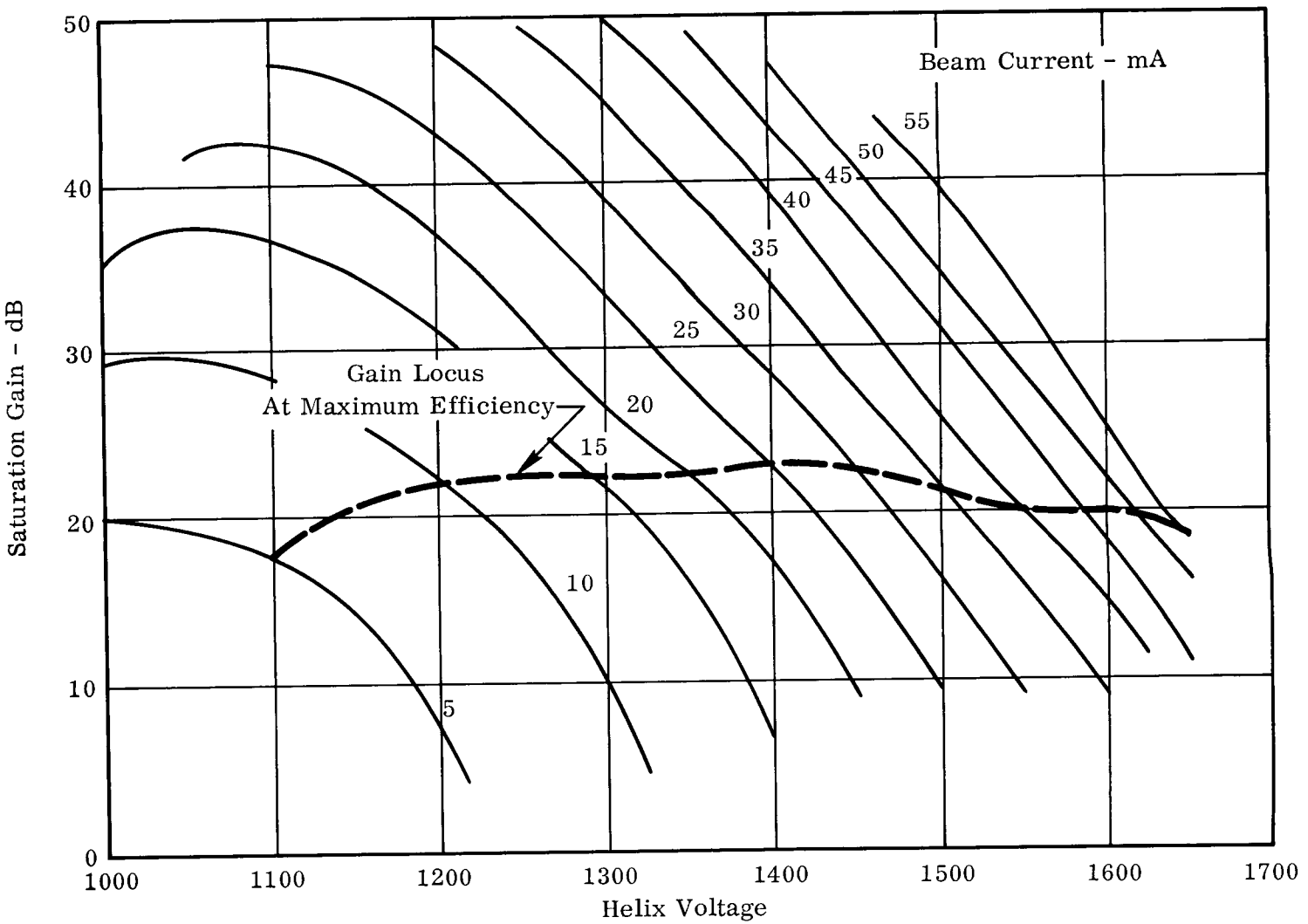

Fig. 3 - Saturation gain versus helix voltage with beam current as the parameter for WJ-274 No. 13 at 2.3 GHz. The gain locus for maximum efficiency is shown.

Figure 4 shows the effect of frequency on beam efficiency at various beam current levels. These data do not correlate exactly with the data of Fig. 2 as they were taken under slightly different conditions. They, however, show that the tube performance is centered at 2.3 GHz.

Figure 5 shows broadband data at a fixed set of conditions. A power output of 25 watts was achieved at an overall efficiency greater than 40 percent over the 200 MHz bandwidth from 2120 to 2320 MHz. The peak overall efficiency, which occurs at 2.3 GHz, reached a value of 41.8 percent. The corresponding beam efficiency is 31.2 percent. Both of the values are realizable after-fade efficiencies taken under CW conditions. The two curves plotted show the importance of the correct adjustment of the magnetic field in the PPM stack. By empirically adjusting the cell values of the magnetic field it was possible to raise the beam efficiency so that the power output increased from 23 to 25 watts. Depressibility of the collector was also improved so that maximum efficiency occurred at a collector voltage of 1060 instead of 1160 volts. Helix current interception only increased 1.0 mA under the maximum efficiency conditions.

Figure 6 shows a power output versus power input characteristic. There is only a 3 dB difference between small signal and large signal gain under best efficiency conditions. This should be compared with tube no. 4, for instance, which was built during the previous development program.[1] That tube contained no positive taper and at conditions which gave 25 watts at this frequency had an 11 dB difference between small signal and large signal gain.

The broadness of the saturation region of the input-output characteristic also improved with the use of the positive taper. This is shown in Fig. 7 . The power output varies no more than 0.5 dB from the maximum for a 4.85 dB variation in drive signal.

Conclusions on WJ-274 No. 13

Some interesting conclusions can be drawn about tube no. 13 and the effect of the positive taper when it is compared with a uniform helix tube. It is compared in Table I with WJ-274 no. 4 which had the best overall performance of the uniform helix tubes developed on the previous program. Tube no. 13 at the 25 watt level is compared with tube no. 4 at the 25 and the 35 watt level.

Note that the beam perveance at the 25 watt level of the two tubes is the same. Experience has shown that this will give approximately equivalent focusing performance.

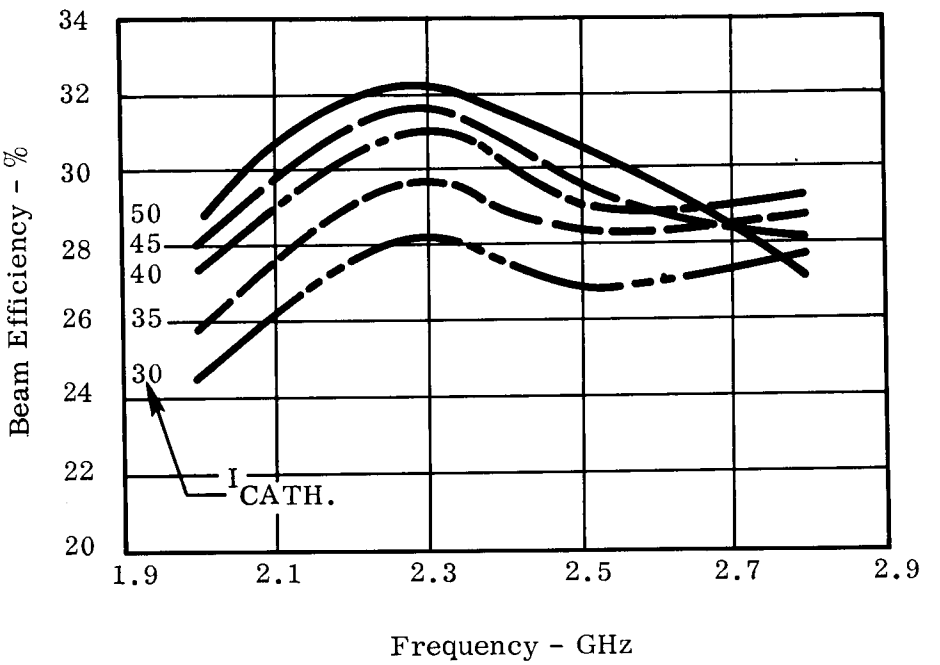

Fig. 4 - Optimized beam efficiency versus frequency for WJ-274 No. 13 for different values of beam current.
17934

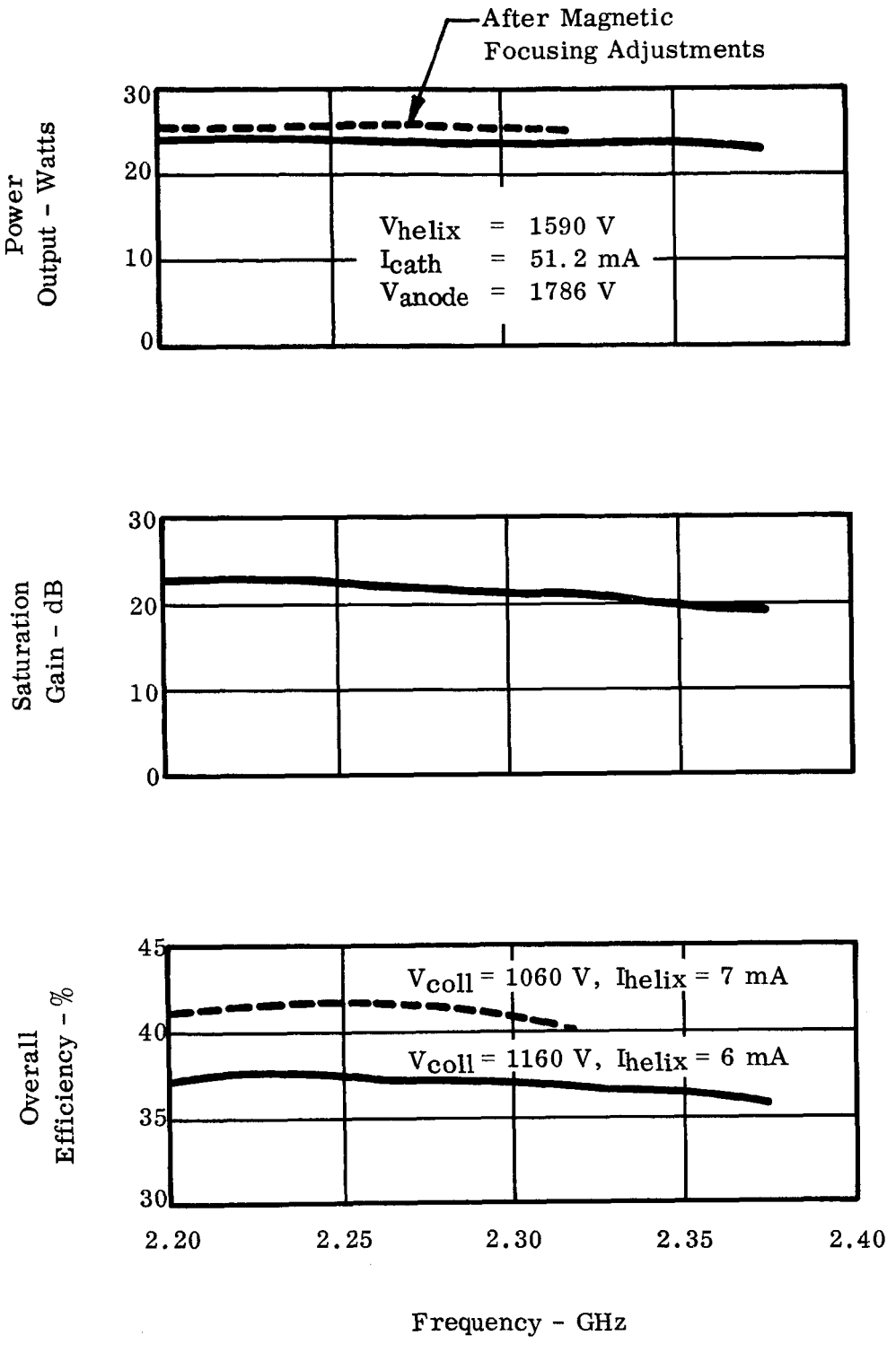

Fig. 5 - Power output, gain and overall efficiency versus frequency for WJ-274 No. 13. The dashed curves were obtained after additional magnet cell adjustments and additional collector depression.

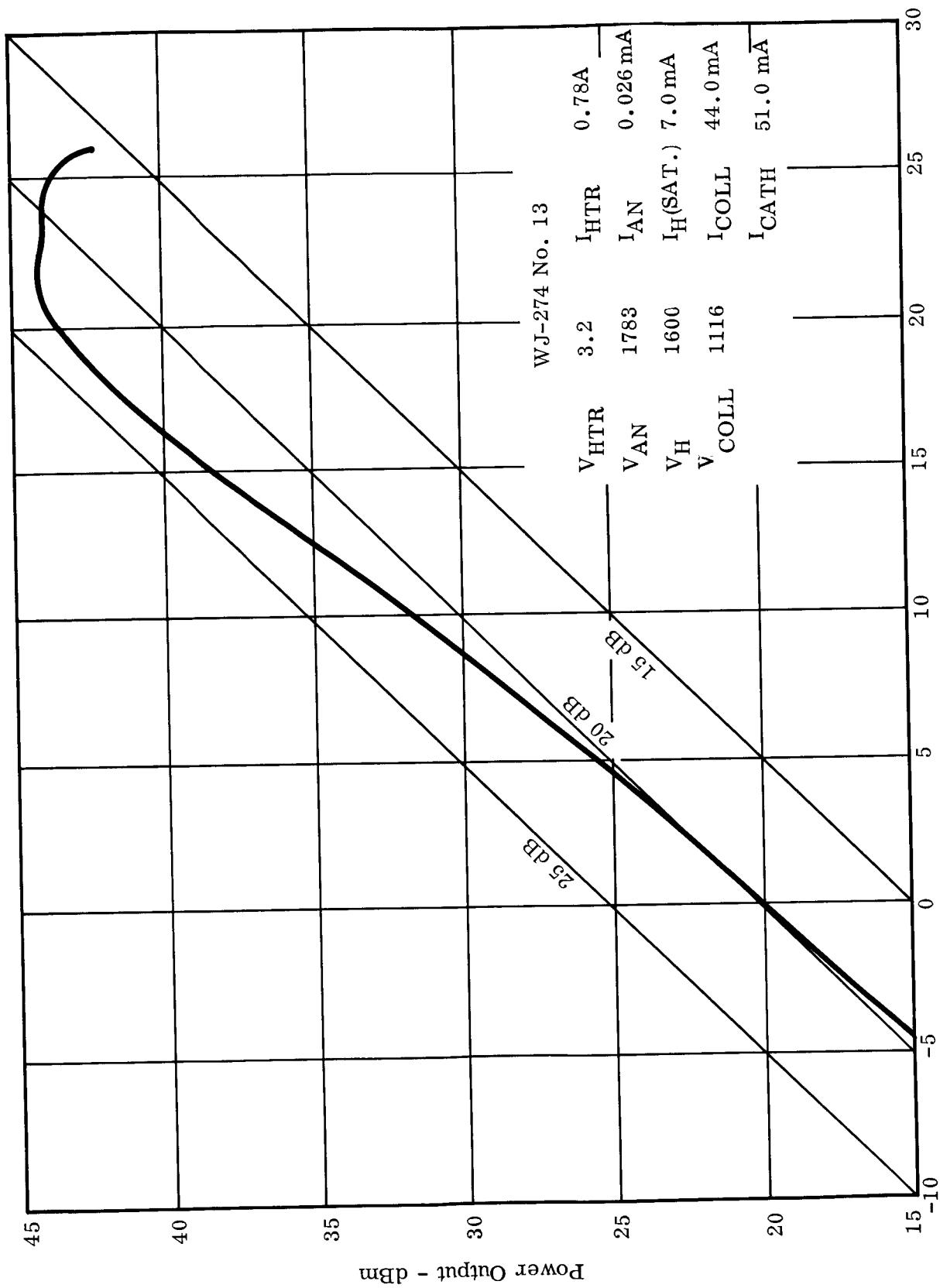

Fig. 6 - Transfer characteristic of WJ-274 No. 13 at 2.3 GHz.

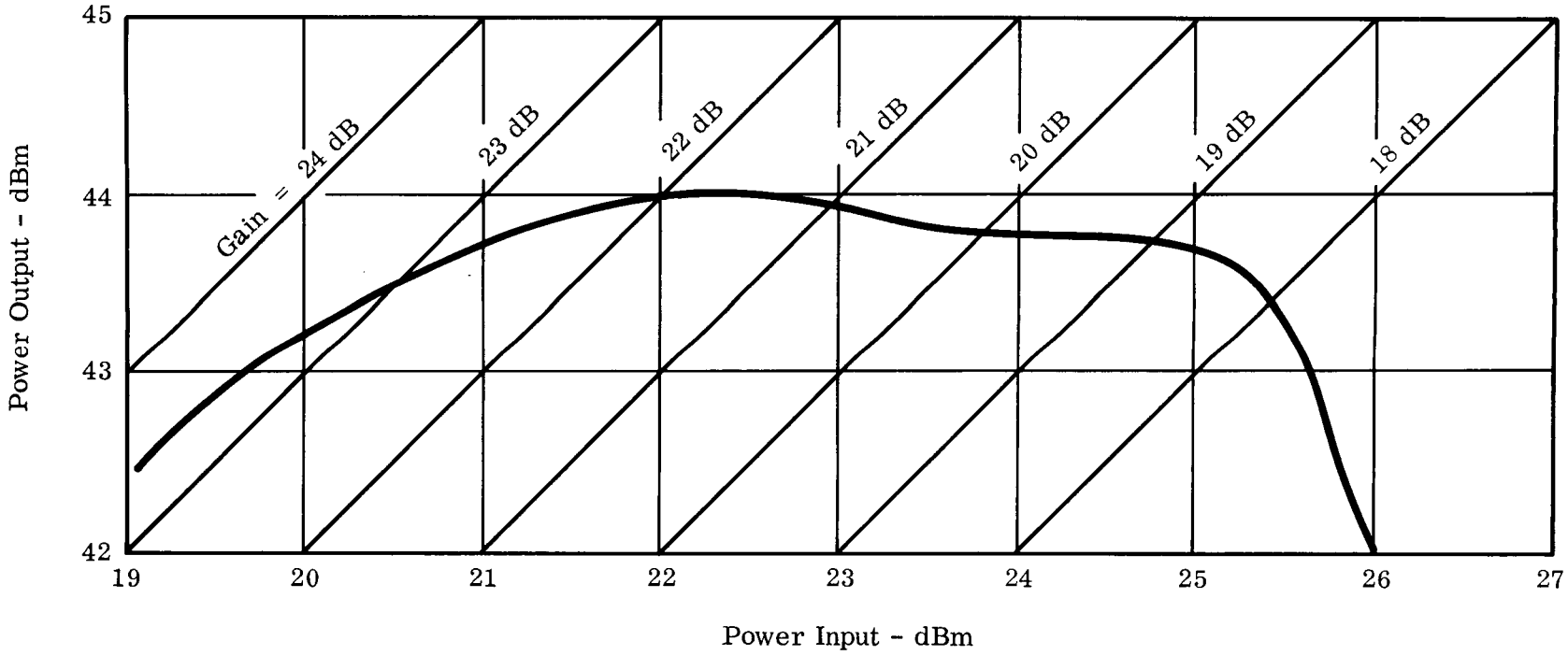

Fig. 7 - Plot of saturation region of the input - output characteristic of WJ-274 No. 13 at 2.3 GHz showing the broadness of this region due to positive tapering of helix. Helix voltage = 1600V. Beam current = 51.0 mA.

TABLE I

COMPARISON OF UNIFORM AND TAPERED HELIX TUBES AT 2.3 GHz

Tube No. RF Power Output Helix Type	No. 4 35 watts Uniform Helix No Taper	No. 4 25 watts Uniform Helix No Taper	No. 13 25.4 watts Positive Taper
$\mathbf{P}_o$ (μ Pervs)	0.960	0.815	0.814
$I_o V_H$ (Watts)	112	87.5	81.5
η_o (%)	31.3	28.6	31.3
η_D (%)	41.5	39.5	43.6
$m = \frac{\eta D}{\eta o}$	1.33	1.38	1.39
V_{Helix} (volts)	1686	1627	1590
I_o (mA)	66.2	53.8	51.2
$V_{Collector}$	1240	1130	1060
$\frac{V_{Collector}}{V_{Helix}}$	0.735	0.695	0.68
I_{Helix} (mA)	11.0	6.0	7.0

$\mathbf{P}_o$ Beam Perveance - $\dfrac{I_o}{V_H{}^{3/2}}$

η_o Beam Efficiency - $\dfrac{P_{RF}}{I_o V_H}$

η_D Depressed Efficiency = $\dfrac{P_{RF}}{V_{AN} I_{AN} + V_H I_H + V_{Coll} I_{Coll}}$

m Efficiency Improvement Ratio

I_o Beam Current = $I_{HEL} + I_{Coll}$

The taper allows tube no. 13 to have a higher beam efficiency (31.3% versus 28.6%) at this power level. In fact, no. 13 has achieved the same beam efficiency at the 25 watt level that no. 4 did at the 35 watt level.

The efficiency improvement ratio due to collector depression is almost identical in no. 13 and no. 4 at the 25 watt level. From this it is seen that the improvement of the depressed efficiency in no. 13 is due entirely to the improvement in beam efficiency.

Even though the same beam efficiency was achieved in no. 13 at 25 watts as in no. 4 at 35 watts, the depressed efficiency was greater in no. 13. Because of the returned electrons to the helix, the collector in no. 4 could only be depressed to 0.735 of the helix voltage for maximum efficiency versus 0.68 of helix voltage for no. 13. This is due to the higher perveance in no. 4 and leads to the higher helix current interception at maximum efficiency.

The use of the taper allows the achievement of higher beam efficiences at lower perveance levels. This has the advantage of allowing greater overall efficiencies to be achieved because of the better depressibility characteristics of the lower perveance beam.

WJ-274 No. 17

The design of WJ-274 no. 17 is patterned after the electrical design of no. 13 with some modifications. As can be seen from Appendix I, it has a slightly longer section following the attenuator and a slightly longer taper section. Its major difference, however, is the 58 TPI input section which operates close to the maximum small signal gain. The gain is improved by 10 dB or more (depending on the exact conditions compared) over tube no. 13.

The major reason for building no. 17 (and also no. 18 which follows) was to try to get around helix loss problems which appeared to be leading to efficiency reduction. The problem became particularly severe on the two-helix tubes (Nos. 14, 15 and 16) because of constructional difficulties. However, loss measurements which could be made on the short attenuatorless helix section in the two-helix tubes indicated that variations in loss were probably resulting in variations in efficiency from tube to tube. As much as four percentage points in variation in efficiency (14% change) has been found on production versions of the WJ-274 known as the WJ-274-1. Looking back on these results and knowing the rigidity of the controls on uniformity from tube to tube, loss variation is the most likely answer to the problem.

The source of this loss and also an explanation to its variability lies in the helix lock-in technique which has been used up to this point. The technique used up through tube no. 16 depended upon the flow of a brazing alloy into the region between the back of a close fitting helix support wedge and the inside of the body of the tube. The alloy used for this purpose contained some silver. Loss remained low during assembly of the tube, but during the bakeout process with a high vacuum inside the tube envelope, the vapor pressure of the silver would allow it to sublime and deposit on the helix wedges in the vicinity of the helix wire. This thin film, depending on the surface resistivity of the deposit, could contribute to a large component of helix loss. This loss in turn would have a direct bearing on the efficiency. The variability could come about from different temperature and internal vacuum levels which would occur from tube to tube during processing. This would result in variations in the deposition rate and thus the resulting helix loss. This loss mechanism was confirmed by constructing and processing short attenuatorless helix sections and measuring loss changes. Loss in excess of 1 dB per inch was measured. It cannot be measured on a conventional tube with internal attenuator. This is why it was not discovered before.

It was reasoned that tube no. 13 might have some residual loss problem despite the fact that it performed well. Comparing its performance to the 1.0 GHz tube from which it was scaled, its power input-output curve was identical except in the region of saturation. This difference could be attributed to loss.

The construction technique for the helix-body section of tube no. 17 was radically changed. The helix was locked-in to the barrel by the triangulation technique of deforming the body, inserting the helix and releasing the body to hold the helix by compression. It required a change in the body material to one which maintained tension on the helix even through the high temperature bakeout cycle. It required changes in the barrel ID and OD to accommodate different fits between helix, body and magnetic pole pieces. In this process, the pole pieces cannot be put onto the body until the helix insertion is complete. They must be loose enough to slide in place which leaves something to be desired from the standpoint of tightness of the pole piece fit to the body. Focusing is bound to be more difficult due to the slight transverse magnetic field components that can occur.

The triangulation technique for helix lock-in to the body eliminates, of course, the need to have any silver containing brazing alloy in the neighborhood of the helix and thus should eliminate any helix loss due to this source. This was checked out in an experimental test where transmission loss was measured through a three

inch section of helix after assembly, after a furnace cycle to brazing temperatures and after a vacuum bakeout to 550° C. Loss was found not to change due to any of the processing.

Tube no. 17 was assembled, processed and placed under test. Figure 8 shows the standard plot of power output, saturation gain and beam efficiency versus helix voltage for three different values of beam current. This was measured at a frequency of 2.3 GHz. The beam efficiency reaches a maximum of 30.7 percent at a current of 50 mA and a helix voltage of 1580 volts. This is within 0.5 percent (or 0.07 dB) of the beam efficiency reached on tube no. 13 and shows that equivalent performance was achieved with an accompanying gain of 30.5 dB, an increase of over 10 dB. These data were taken under peak magnetic field conditions of 1000 gauss.

Figure 9 shows performance versus frequency with current and voltage fixed. It is seen that the frequency of optimum efficiency is 2.2 GHz at the 50 mA condition. The peak beam efficiency obtained is 31.8 percent, which exceeds that of tube no. 13. Again it is seen that careful optimization of the magnetic field program leads to improved power output and efficiency. The longer output helix sections on tube no. 17 appear to have shifted the peak efficiency point toward lower frequencies. This same effect of the shift toward lower frequencies has been observed on other high efficiency tubes with longer output helix sections.

Note that beam efficiency is plotted in Fig. 9 instead of overall efficiency. This is done because of the poor focusing characteristics of this particular tube and the resulting inability to depress the collector voltage very much. The focusing is poor because of the type of pole pieces used and the fact that they were not tight to the tube body. These pole pieces are die-punched parts brazed back to back instead of the machined pole pieces used on tube no. 13. This type of pole piece had been successfully used on tubes where the pole pieces were brazed to the body. In the case encountered in tube no. 17 where the pole pieces are slid on over the triangulated body, even though they fit very snugly after assembly they were loose after bakeout. They were tightened by deforming the hubs with a special tool, but this did not make them sufficiently tight. The machined pole piece, because of its greater inherent mechanical strength, does not loosen during bakeout and with the proper treatment of the surfaces involved can be made to stick firmly to the body by a diffusion-weld during bakeout. This latter effect makes the focusing adjustments on the tube very much simpler and makes the focusing much more stable.

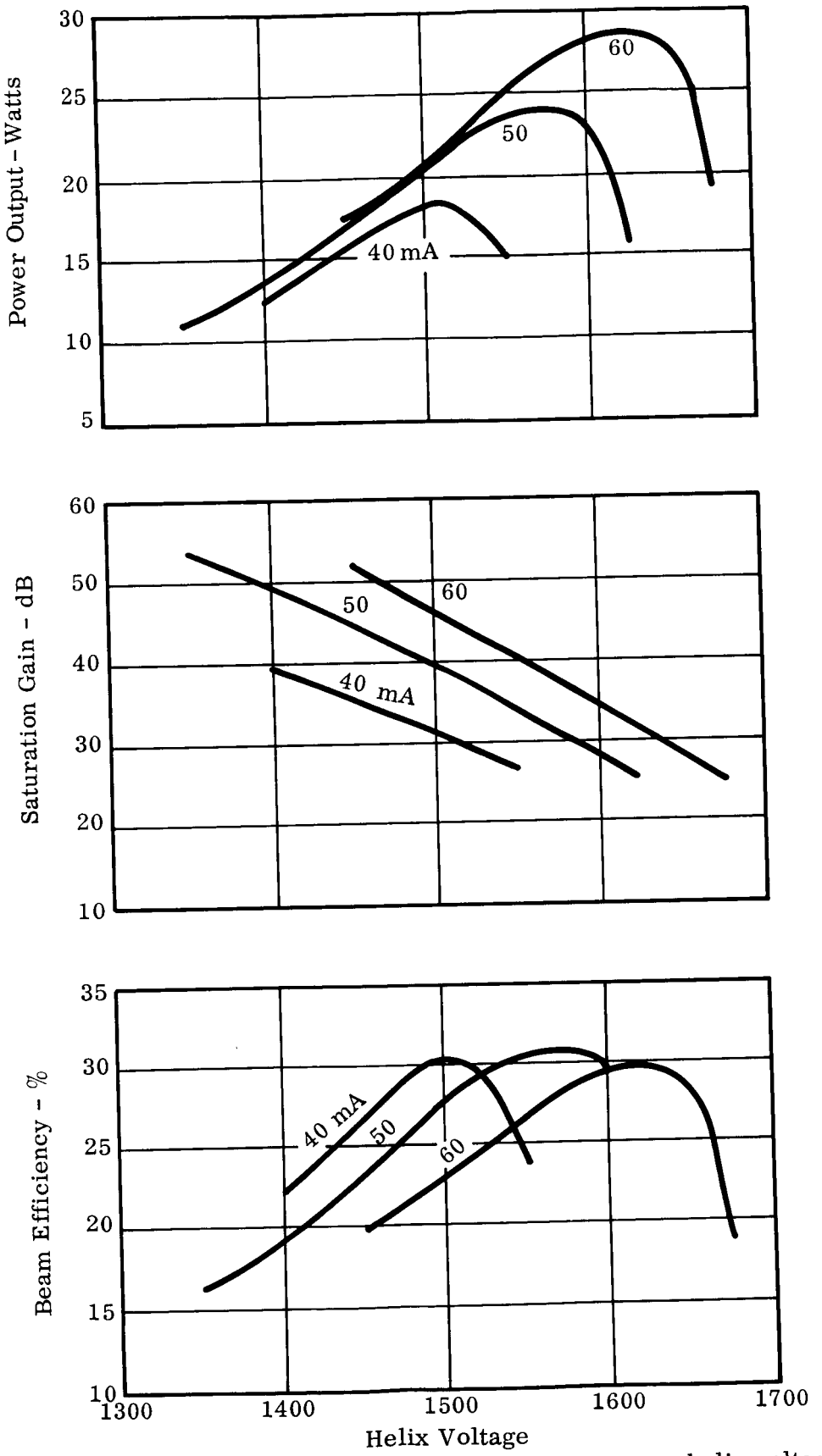

Fig. 8 - Power output, saturation gain and beam efficiency versus helix voltage with beam current as the parameter for WJ-274 No. 17. Frequency = 2.3 GHz.

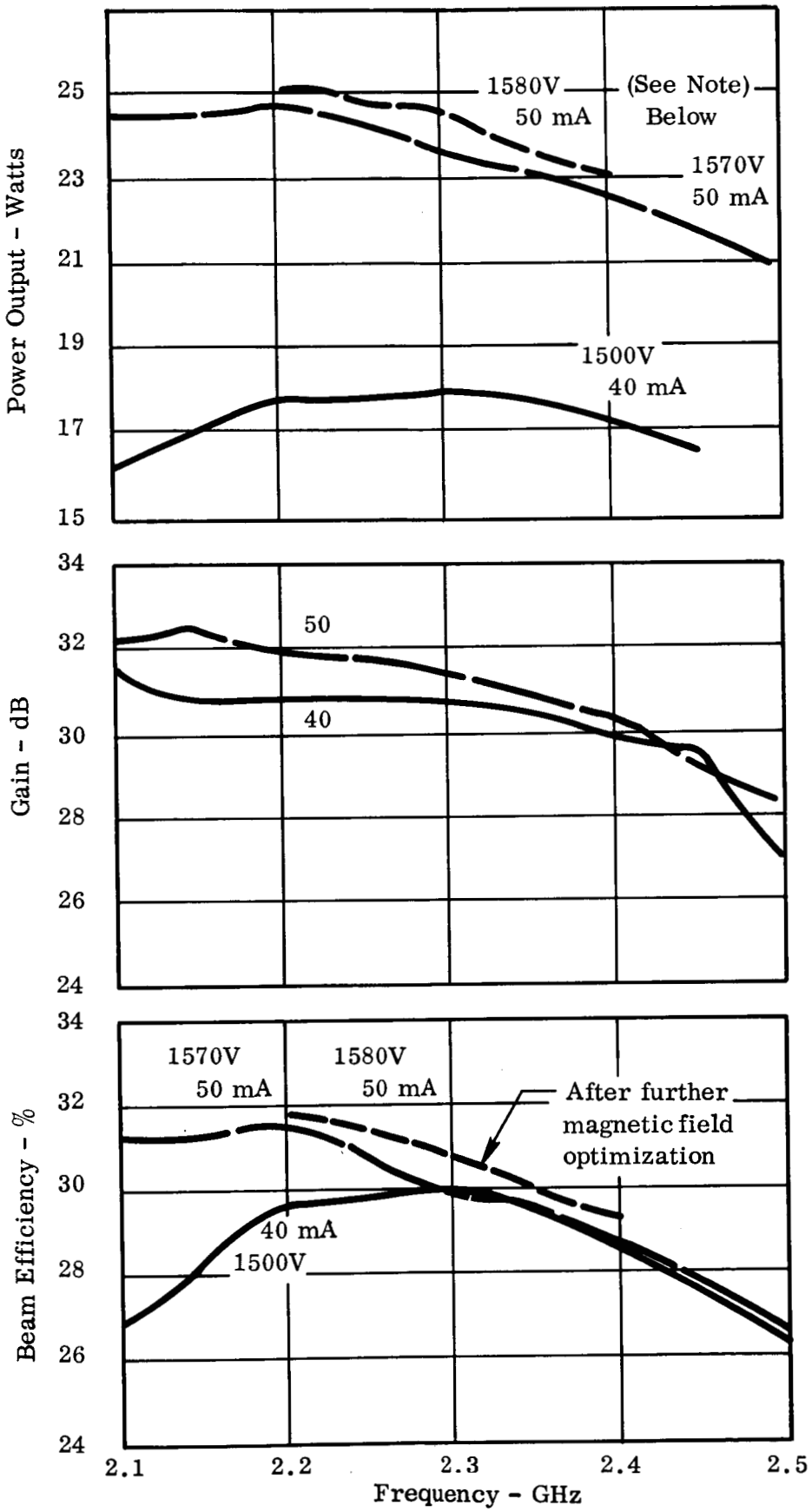

Fig. 9 - Power output, gain and beam efficiency versus frequency for WJ-274 No.17.

Figure 10 shows an input-output power curve at two different beam currents. It is similar to tube no. 13 in that it shows a large improvement over that of a uniform helix tube. The small signal and saturation gain differ by 7 dB in the 50 mA case. In the saturation region, the width of the response 0.5 dB down from the maximum is 4.4 dB under the same conditions. Both of these characteristics are not quite as good as no. 13. The saturation width is only 0.45 dB narrower while small to large signal gain change is 4 dB greater. This latter characteristic is not important to high efficiency tubes except that it appears to be related to the 0.5 dB saturation width.

Conclusions on WJ-274 No. 17

This tube demonstrated a slightly higher beam efficiency than tube no. 13, but this maximum efficiency point has moved 100 MHz down in frequency to 2.2 GHz. At 2.3 GHz, the efficiency is within 0.5 percentage points of no. 13. The slightly higher beam efficiency at 2.2 GHz probably indicates only a slight improvement in the helix loss situation. This means that no. 13 has little additional loss due to evaporated silver over the basic loss of the helix. No. 17 has shown a slightly narrower "0.5 dB saturation width."

The real improvement demonstrated with no. 17 is the ability to increase the gain of the tube by over 10 dB without degradation to the beam efficiency. The tube can now meet the 30 dB gain minimum requirement.

It is felt that the poorer focusing properties of tube no. 17 is due entirely to the poorer magnetic circuit properties. The helix interception current under dc conditions as well as the helix interception under drive with no depression both indicated bad beam transmission. This latter interception was 12 mA and under normal situations which result in good depression there is only 3 mA interception. There was a problem on assembly which led to both loose pole pieces and non-uniform period in some cells. This is a correctable problem. The inability to depress the collector potential with low helix interception is directly attributable to focusing problems.

WJ-274 No. 18

The design of WJ-274 No. 18 is again patterned after the electrical design of no. 13 with some modifications. As can be seen from Appendix I, no. 18 is more like tube no. 13 than no. 17 primarily because it has the same TPI for the helix

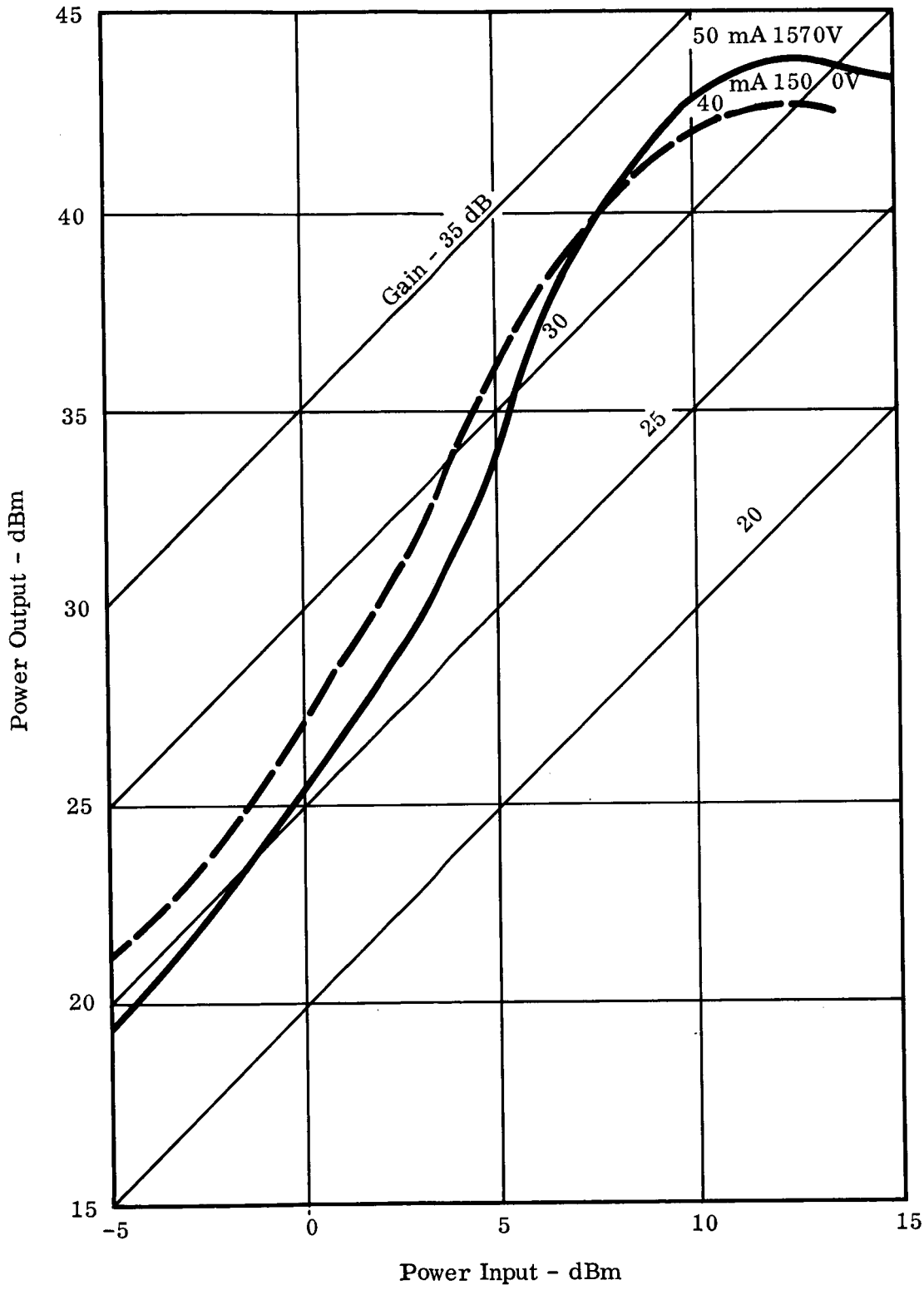

Fig. 10 - Input - output curves for WJ-274 No. 17 at 2.3 GHz.

sections ahead of and following the attenuator. It also has the same length taper section as no. 13. The tube nos. 17 and 18 were essentially built simultaneously so that the design of one could not be based on the results of the other. Instead, alternative designs based upon no. 13 were chosen. Tube no. 18 was also constructed with the triangulation lock-in technique for the helix. The same pole piece problem exists on this tube as on no. 17, however the problem in non-uniform magnet period was corrected. Focusing performance has been considerably improved on this tube but it is still not as good as on no. 13. As a result the depressibility is much better than no. 17 but still does not match no. 13.

Since tube no. 18 does not have the synchronous input sections of helix, it is not expected to have as high a gain as tube no. 17.

Figure 11 shows the standard plot of power output, saturation gain and beam efficiency versus helix voltage for several values of beam current. It is seen that the beam efficiency of 32.2 percent at 2.3 GHz exceeds that of tube no. 17 and is also better than the after fade beam efficiency of tube no. 13 which was 31.8 percent. Saturation gain at maximum efficiency is 29 dB. At 50 mA and 1550 volts the power output is just 25 watts. Data were taken also with the magnet stack changed to a peak magnetic field of 1050 gauss. The effect of this was to lower power and beam efficiency. The effect of the magnetic field change on gain was negligible.

The implication that better beam efficiency might be obtained by lowering the peak magnetic field to 950 gauss was not explored but offers a good possibility.

Figure 12 shows the plots of power output, saturation gain and beam efficiency versus frequency. In this tube, the beam efficiency peaks in the frequency range between 2.3 and 2.4 GHz. It goes as high as 33.0 percent at a beam current of 60 mA.

Figure 13 shows the input-output power curves at the 40 and 50 mA values of beam current. The 50 mA curve exhibits only a 4 dB difference in gain between small signal and saturation gain. This also leads to a broad top on the curve in the saturation region. The "0.5 dB saturation width" allows a 5 dB variation in drive power. This is better than tube no. 13.

Figure 14 shows the collector depression characteristic. Under the 1000 gauss conditions, the overall efficiency rises to slightly over 40 percent. With the higher beam efficiency that this tube exhibits, it would reach a higher overall efficiency

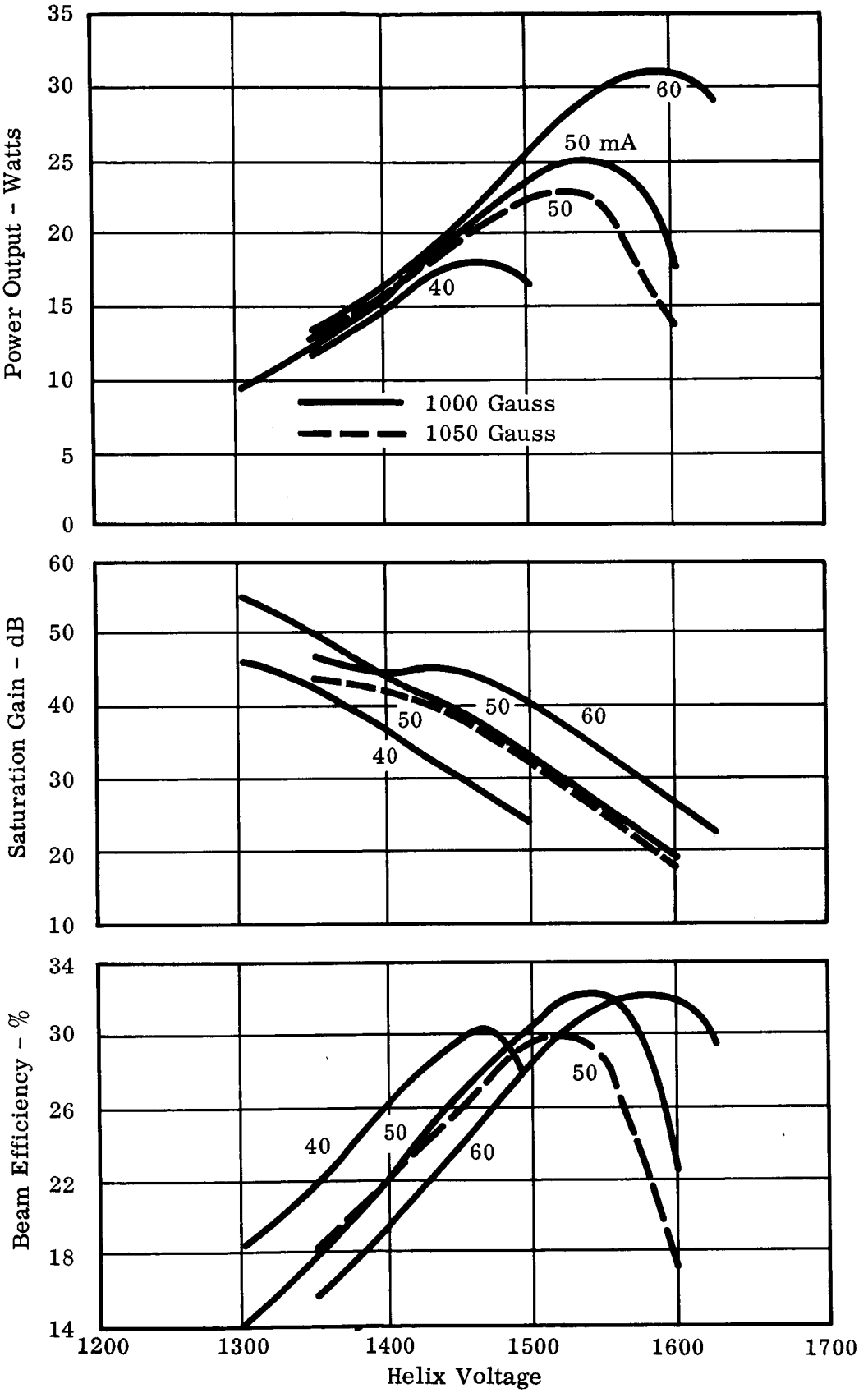

Fig. 11 - Power output, saturation gain and beam efficiency versus helix voltage for WJ-274 no. 18. Frequency = 2.3 GHz.

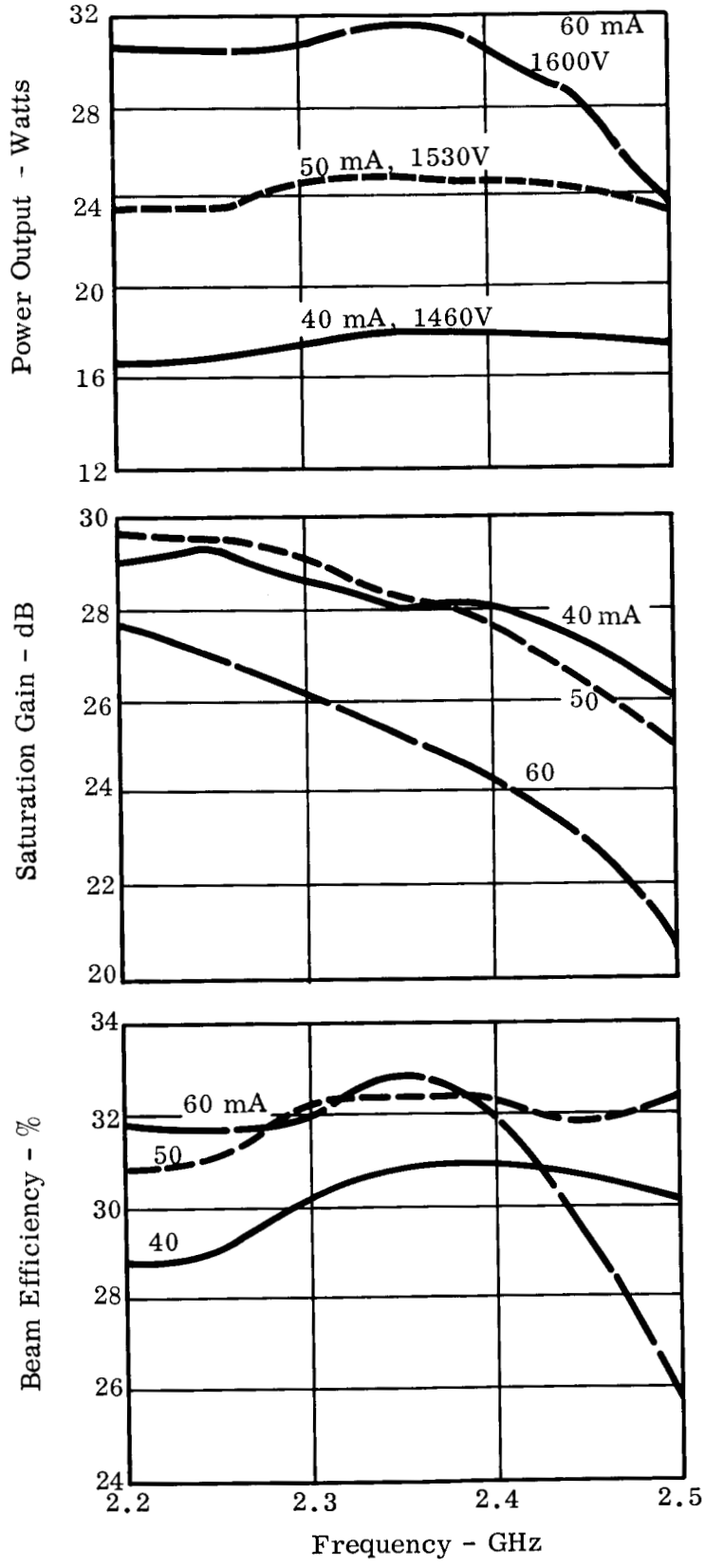

Fig. 12 - Power output, saturation gain and beam efficiency versus frequency for WJ-274 No.18.

17939

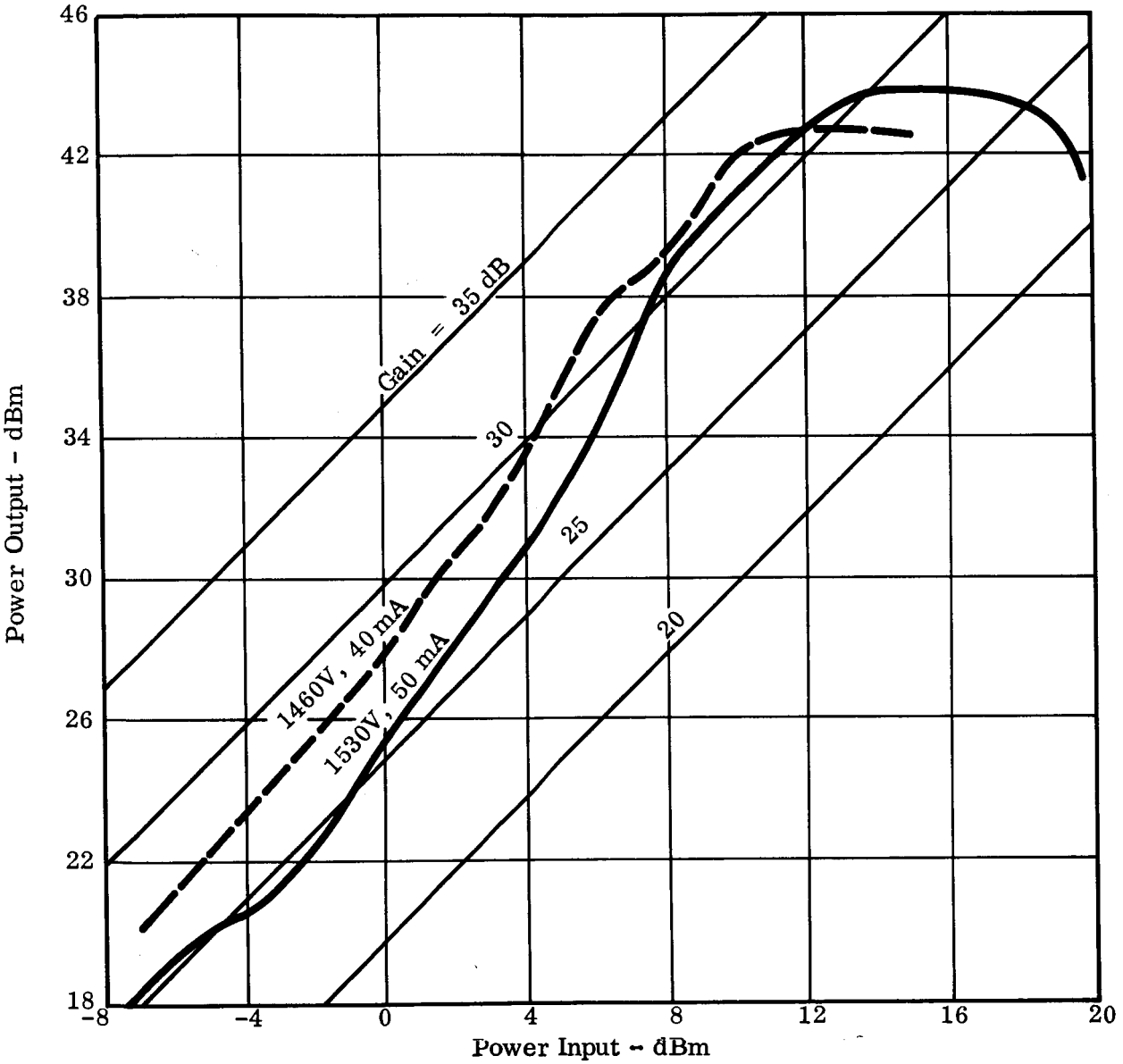

Fig. 13 - Input - output curves for WJ-274 No. 18 at 2.3 GHz.

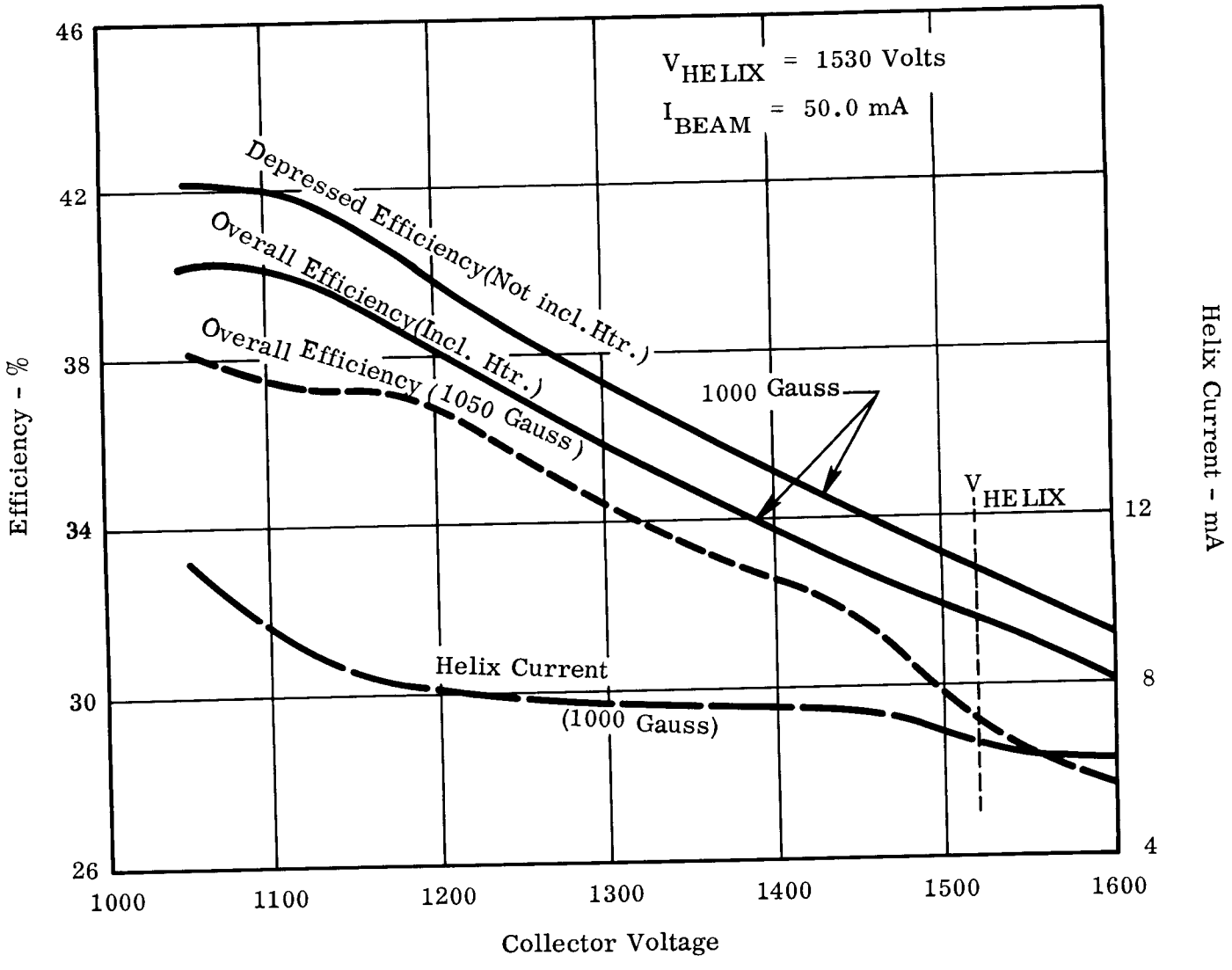

Fig. 14 - Collector depression characteristic showing efficiency versus collector voltage for the WJ-274 No. 18 at 2.3 GHz. The effect of peak magnetic field is shown.

if the primary helix current interception were not so high. Helix current interception in the collector voltage region between 1200 and 1400 volts represents the current intercepted on the helix due to RF defocusing as the beam passes through the large signal section at the output end of the helix. Under these conditions, it should be 3 to 4 mA. Because of the magnetic field problems, 7.5 mA was the minimum primary interception that could be achieved. The rise in helix current below 1200 volts is due to reflected electrons from the collector and determines the lower limit to which the collector voltage can be depressed.

Figure 14 also shows the effect of the higher peak magnetic field in the PPM stack. It decreases the beam efficiency which in turn lowers the overall efficiency. The rate of change of efficiency with collector voltage is about the same at either value of magnetic field.

Conclusions on WJ-274 No. 18

Tube no. 18 has exhibited the best beam efficiency at the 25 watt level of any of the positive taper design tubes. If it had not exhibited focusing problems due to the change in the pole piece and construction technology, it would have been the tube with the highest overall efficiency. The depressed efficiency (not including heater) could possibility have gone as high as 44 percent. In addition, this tube exhibited the broadest saturation region of any of the tubes built on the program.

WJ-274-6 No. 2

This tube is being reported here even though it was not built on this program. This is a tube being built for the Jet Propulsion Laboratory on a fixed-price contract. It was to be built using the best design resulting from this Langley Research Center development program. The design of the tube used the input helix design of tube no. 17 and the output helix design of tube no. 13. It incorporated some mechanical improvements to overcome the loose pole pieces and magnet problems of nos. 17 and 18. The pole pieces were locked onto the body of the tube so that no rotational motion was allowed. These changes led to extremely good focusing performance and this tube has given the best efficiency performance yet seen with the WJ-274 tube type.

The plots of power output, saturation gain and beam efficiency are shown in Fig. 15. At 25.7 watts, gain is 34 dB and beam efficiency 32.5 percent. This represents best achieved performance on any WJ-274 to date.

Figure 16 shows power output, saturation gain and overall efficiency versus frequency. Power output and gain are seen to be very flat across the range 2.2 to 2.3 GHz. Overall efficiency lies between 41 and 42 percent from 2.110 to 2.390 GHz.

Figure 17 shows the depression characteristics of the collector with helix current remaining below 7.5 mA at maximum efficiency. The depressed efficiency before accounting for heater power reaches 44.3 percent.

The input-output curves are shown in Fig. 18. Note that the small signal gain lies within the gain values across the saturation region. The power input range corresponding to 0.5 dB decrease in power output is 5.0 dB.

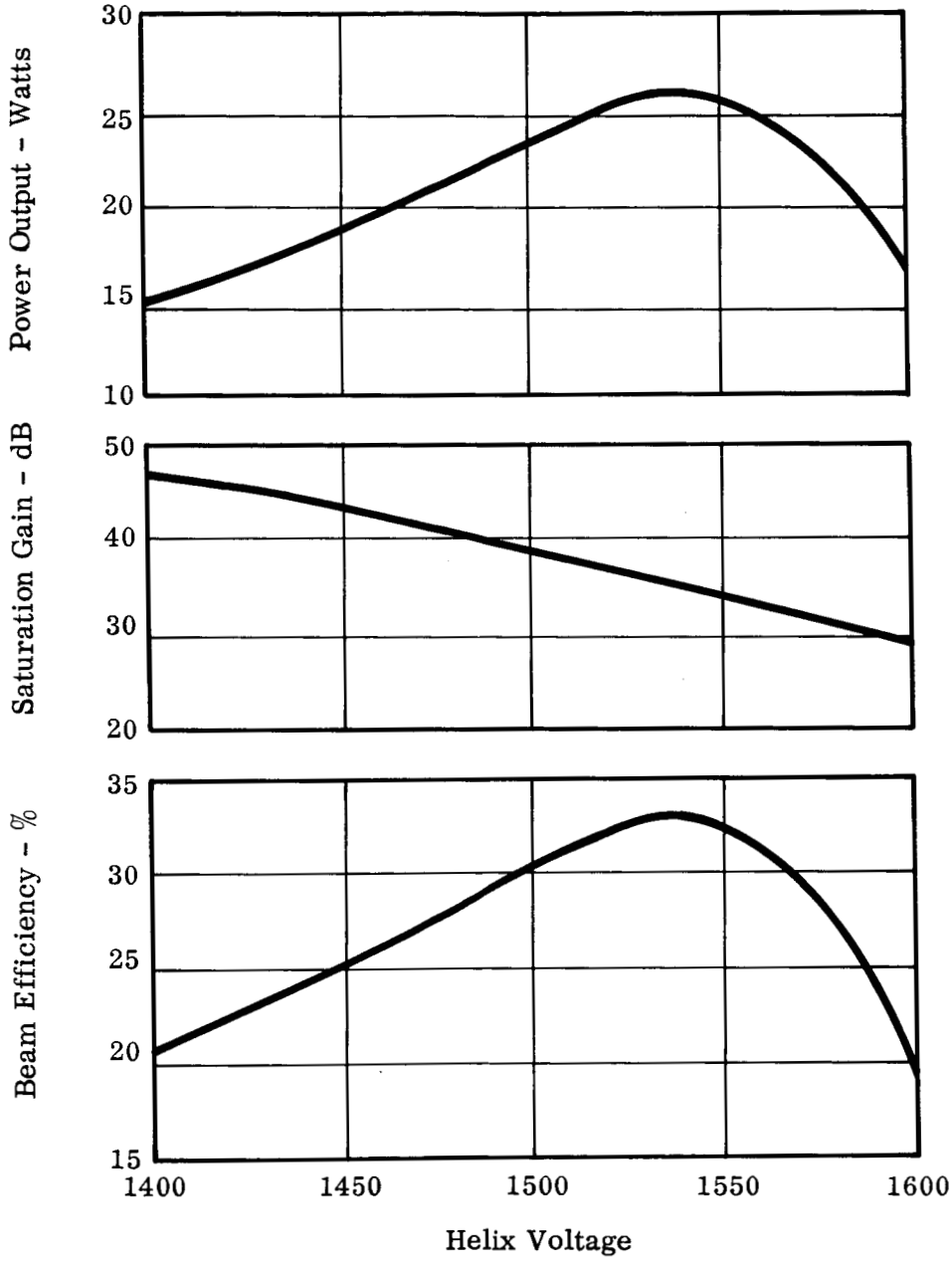

Fig. 15 - Power output, saturation gain, and beam efficiency versus helix voltage for WJ-274-6 No. 2. Frequency is 2.3 GHz and beam current is 51.0 mA.

17985

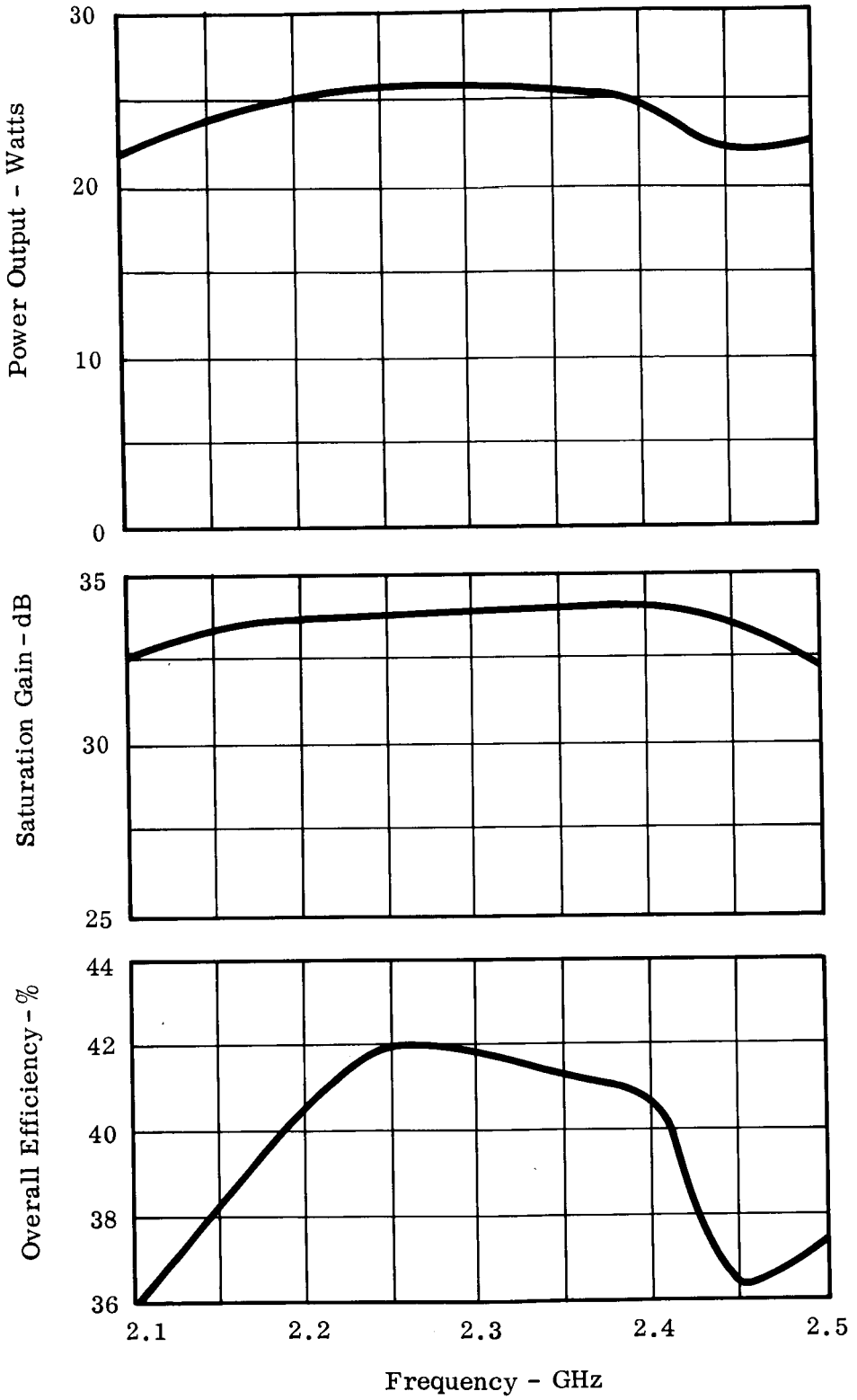

Fig. 16 - Power output, saturation gain and overall efficiency for WJ-274-6 No. 2 versus frequency. Helix voltage = 1550V; Beam current = 51.0 mA.

17986

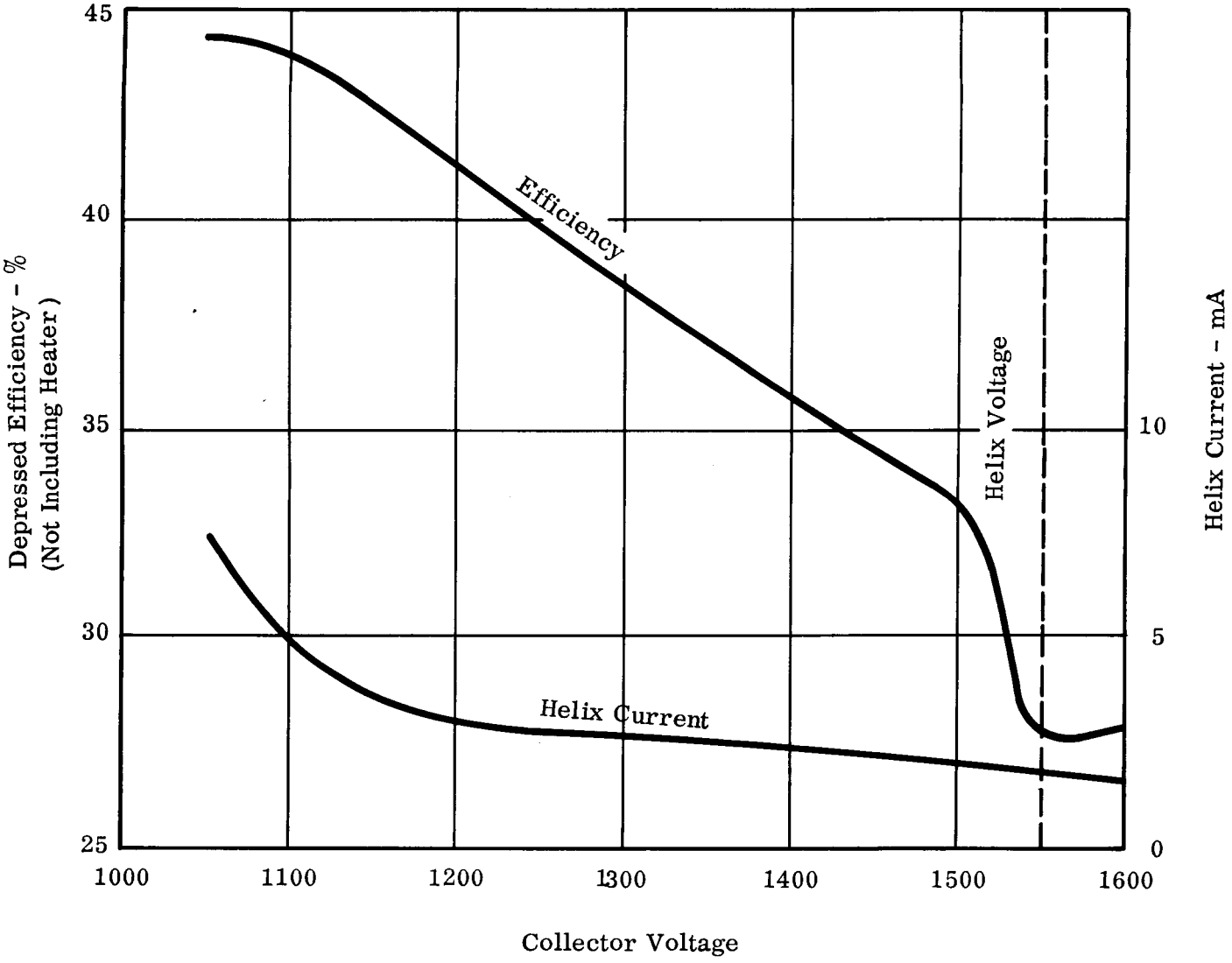

Fig. 17- Depressed collector characteristics for WJ-274-6 No. 2.Helix Voltage = 1550V, Beam Current = 51.0 mA, Beam Current = 51.0 mA, Frequency = 2.3 GHz.

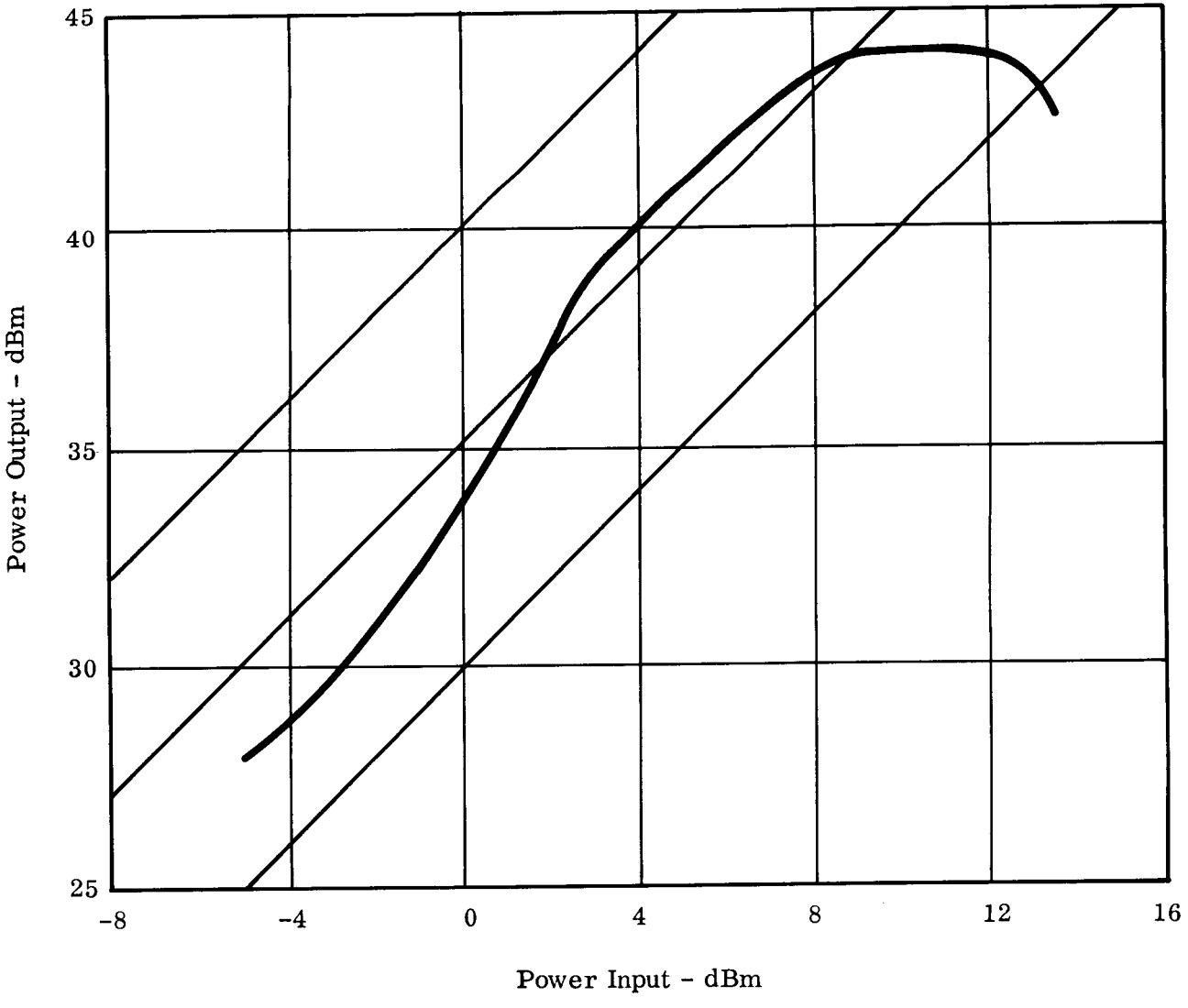

Fig. 18 - Transfer curve of WJ-274-6 No. 2. Helix voltage = 1550V, Beam current = 51.0 mA, Peak magnetic field = 970 gauss.

III. TWO-HELIX TUBES

Design Basis for the Two-Helix Tubes

The design of the two-helix tubes are based upon scaled designs of the Niclas-Gerchberg two-helix tubes built on the USAECOM High Efficiency Study Program. In actuality this turns out to be very similar to the design of WJ-274 no. 13 if the positive taper section is separated from the rest of the helix and operated independently. The helix designs are shown in Appendix I and correspond to tube nos. 14, 15 and 16. The first helix section is designed to operate at a perveance of 0.8×10^{-6} and the second section will be at a lower perveance. It is intended that the operating voltage of second helix be explored experimentally to determine its best operating conditions. From the results of Niclas-Gerchberg, it was known that the second helix should operate at a voltage which was higher than the first, corresponding to an increasing voltage jump.

The physical layout of the tube is shown in Fig. 19. The first helix section is actually made up of two separate helix circuits with their own center terminations. Since this combination can be run as a separate tube with its own input and output terminals, it is referred to as the "first helix". Because this first helix section is made up of two independent helices it is easy to construct the input and output terminals to be physically oriented at right angles with respect to one another. It can be seen from Fig. 19 that this eliminates interference between connectors that would occur if the output terminal of the first helix and the input terminal of the second helix were parallel to one another. The two connectors of the second helix are oriented in line because this is one continuous helix and relative orientation restrictions occur because of the location of the helix support wedges. It is easier in this case to put the connectors in line.

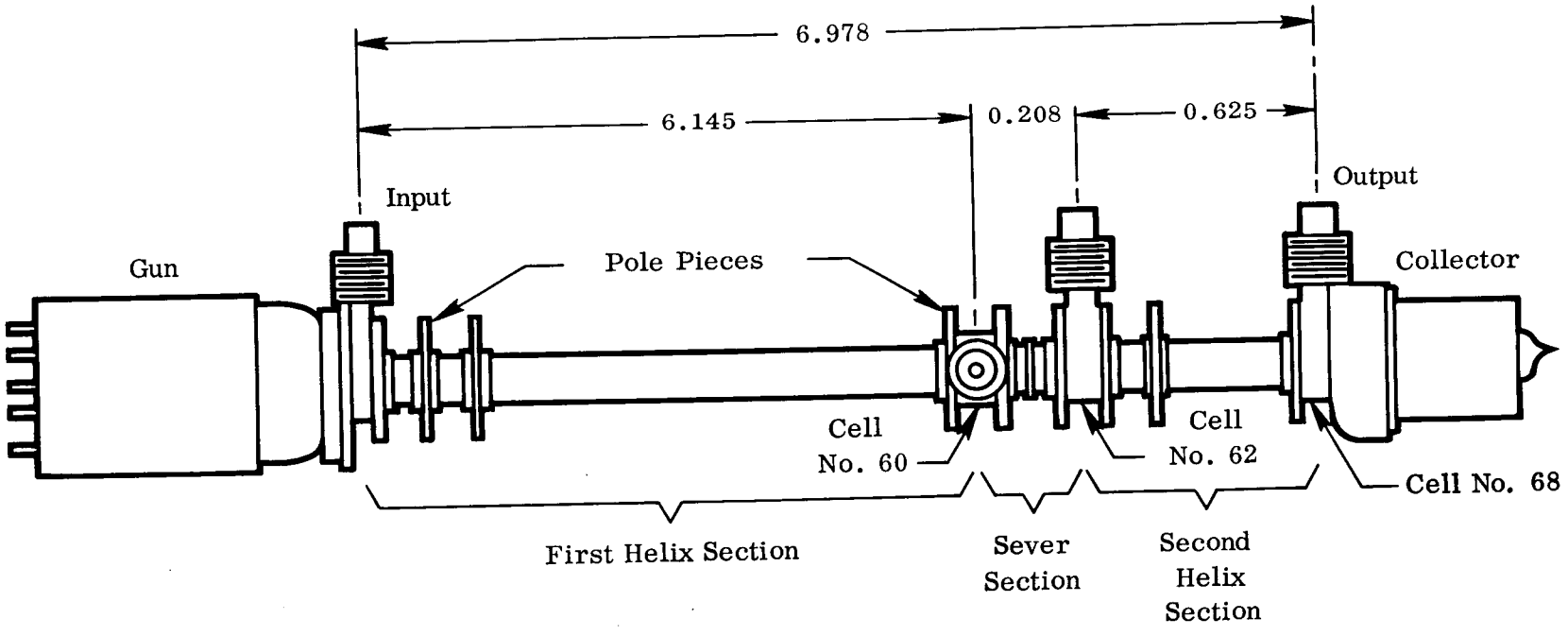

Note: For clarity, most of magnet stack pole pieces have been eliminated from the drawing.

Fig. 19 - Sketch showing dimensions and configuration of two-helix tubes built on the program. These dimensions correspond to Tube No. 14.

The tube is constructed by first independently building the first helix section and the second helix section. These are then joined at the sever and the gun and collector subassemblies are added last.

Problems Encountered on the Two-Helix Tubes

Several problems were encountered with tube no. 14 , the first two-helix tube constructed. Some of these problems involved the construction and some involved the RF characteristics. The construction of the tube turned out to be much more time consuming and difficult than anticipated. To correctly solve the constructional difficulties would require different constructional techniques.

The RF problem which was most detrimental to tube performance was the helix loss problem. This occurred during brazing assembly and vacuum bakeout of the tube. Because of the difficult heating problem during the bell-jar braze at the sever, the body was overheated and an excess of the silver-bearing brazing alloy flowed into the interior of the tube. A cross-sectional view of the sever region is shown in Fig. 20. The left-hand and right-hand sections are aligned with a metal part indicated as the sever joining segment. This was then brazed in place by a radiation heater placed around this joint which raises the temperature of these parts until the brazing alloy, which fits in the two grooves shown, melts and fills the joint. This is a standard technique used under many different situations to successfully join two tube body halves at the attenuator sever. This joint, at a typical body sever in the center of an attenuator, is fairly well thermally isolated since only the thin body wall and the sever joining segment need be heated. However, the situation shown in Fig. 20 is more complicated. The adjacent pole pieces and the outer conductors of the striplines represent a considerable heat sink. It was found that to bring the joint up to the melting point of the brazing alloy it was necessary for a much longer application of heat to accomplish this braze. Since the helices are already mounted in the body assemblies at this time, it subjects them to excessive temperature and the possibility of flowing excess alloy down the barrel and around the helix region. Later transmission loss measurements on the short attenuatorless output helix sections showed that helix loss increased even during hydrogen furnace heating cycles in the presence of excessive alloy.

A further source of helix loss occurred during the vacuum bakeout when the internal tube pressure decreased to the point where it was less than the vapor pressure of the silver bearing alloys. The silver metal sublimed onto the helix wedges further increasing the loss and caused leakage resistance between the second helix section and the body of the tube. On tube no. 14, a 10K leakage resistance appeared after processing of the tube. This was arced off using a high voltage supply so that the tube could at least be operated.

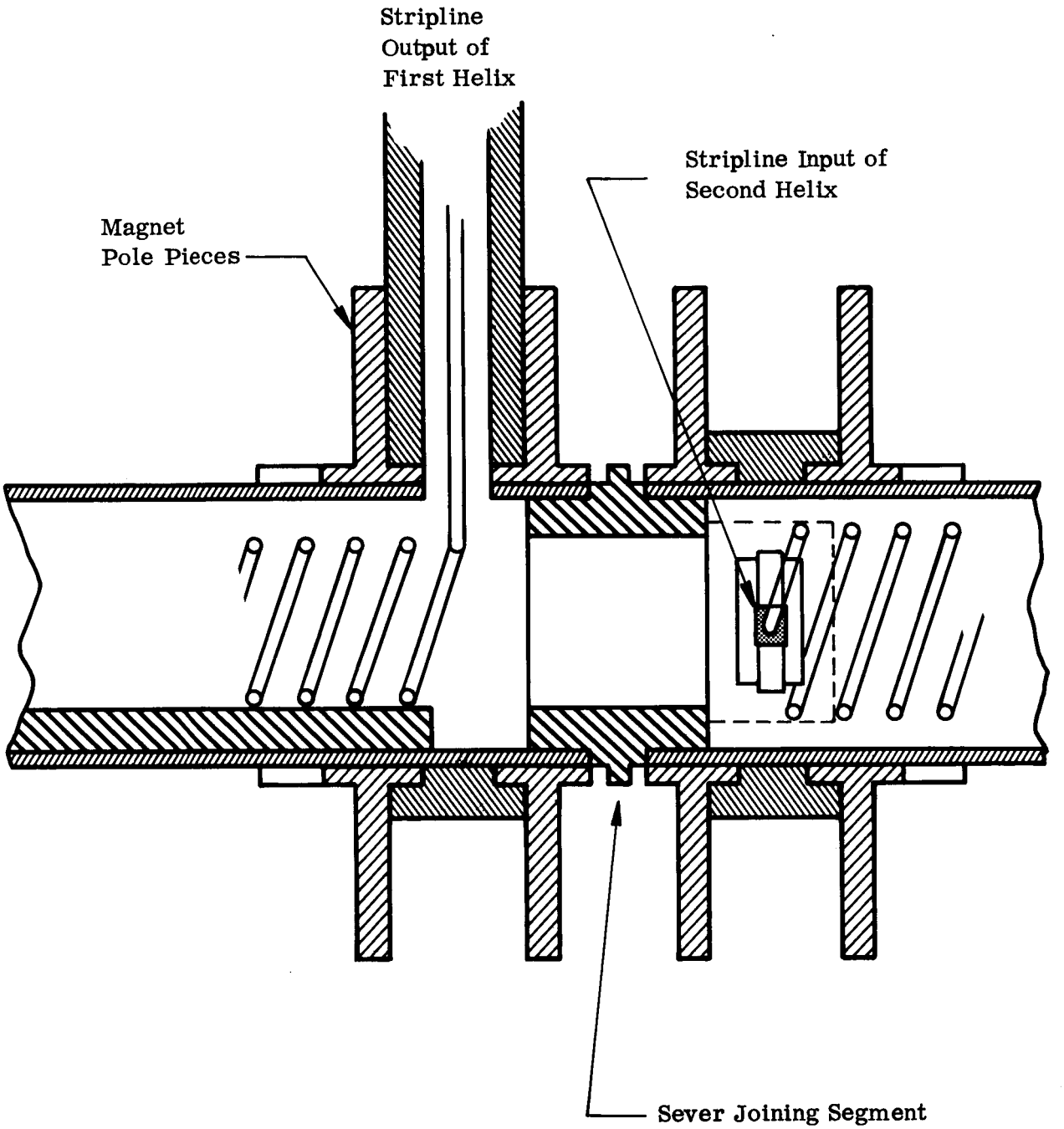

Fig. 20 - Sketch of sever section showing relative location of output and input of first and second helices. There is a 90° relative orientation of these two striplines.

16648

Further measurements of the RF loss of the second stage helix showed it to have an attenuation of 1.4 dB where a loss of only 0.25 to 0.30 dB was expected.

Figure 21 shows power, gain and efficiency performance of the first helix section of tube no. 14 alone. With this helix design, this section alone should have produced 20 watts at a beam efficiency of 27 percent. It is seen that due to the large value of helix loss, the performance is far below normal with a peak beam efficiency of 12.2 percent and a power output of 8.9 watts. With voltage difference applied between the helix sections, it was found that second helix current interception increased very rapidly with the difference voltage. Power output also decreased with increased second helix voltage. This was not expected and did not correspond to the results on the two-helix tubes of Gerchberg and Niclas. This may be due to the large helix loss.

Tube no. 14 was partially dismantled to the extent of removing the gun and collector subassemblies. An organic etching solution composed of formic acid and hydrogen peroxide followed by ammonium hydroxide and hydrogen peroxide was passed through the body in the helix region. This was in an attempt to remove the deposited metals on the wedge surface. These solutions were subsequently washed out in an ultra-clean alcohol bath. Any remaining microscopic quantities completely breakdown in a vacuum under temperature into nitrogen, carbon dioxide, water vapor, and oxygen and leave no residues harmful to the cathode.

Tube no. 14 was retested and gave results shown in Fig. 22. This is even poorer performance than that shown in Fig. 21. Output power of both helix no. 1 and no. 2 are shown. Evidently, the loss problem was only made worse. These tubes showed a power fade after application of RF drive of 1.6 dB. This is a very large value and shows the extent of the problem. The measurement setup used in these tests is shown in Fig. 23.

WJ-274 No. 15

The assembly techniques were changed on this tube to allow for furnace brazing of the two helix sections together rather than using the bell-jar brazing technique. This method should prevent overheating of the body-helix structure in the neighborhood of the sever because of the better temperature control that can be accomplished in the furnace. It would have to be a dry hydrogen braze, however, so that the tube attenuator would not be deteriorated.

Construction of the tube proceeded to the point where the two helix sections were to be joined by the furnace braze in dry hydrogen. The lock-in of the helix to the body was to occur at the same time. During the braze, the output of the first helix section

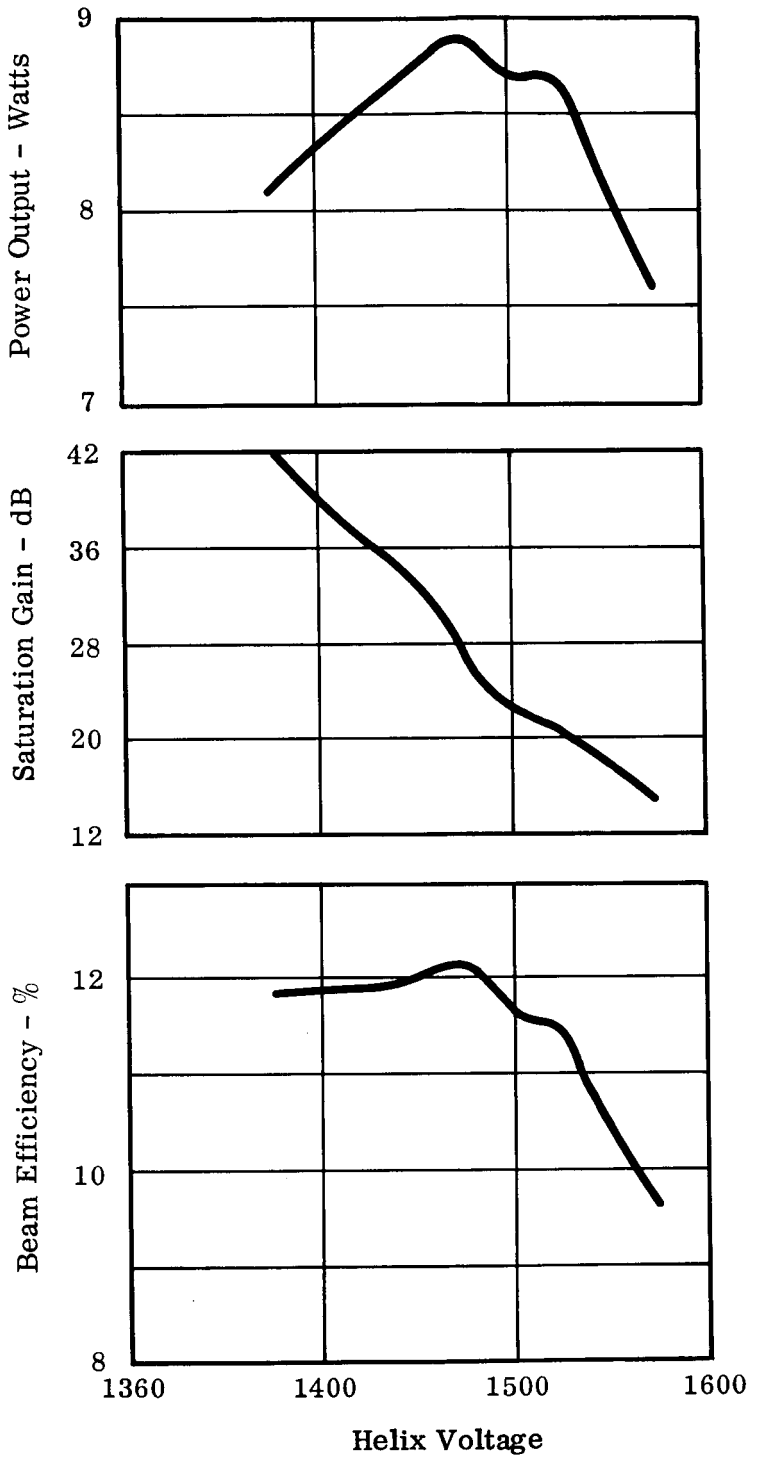

Fig. 21 - Measurements on WJ-274 No. 14 showing performance of first helix section alone. Beam current = 50 mA.

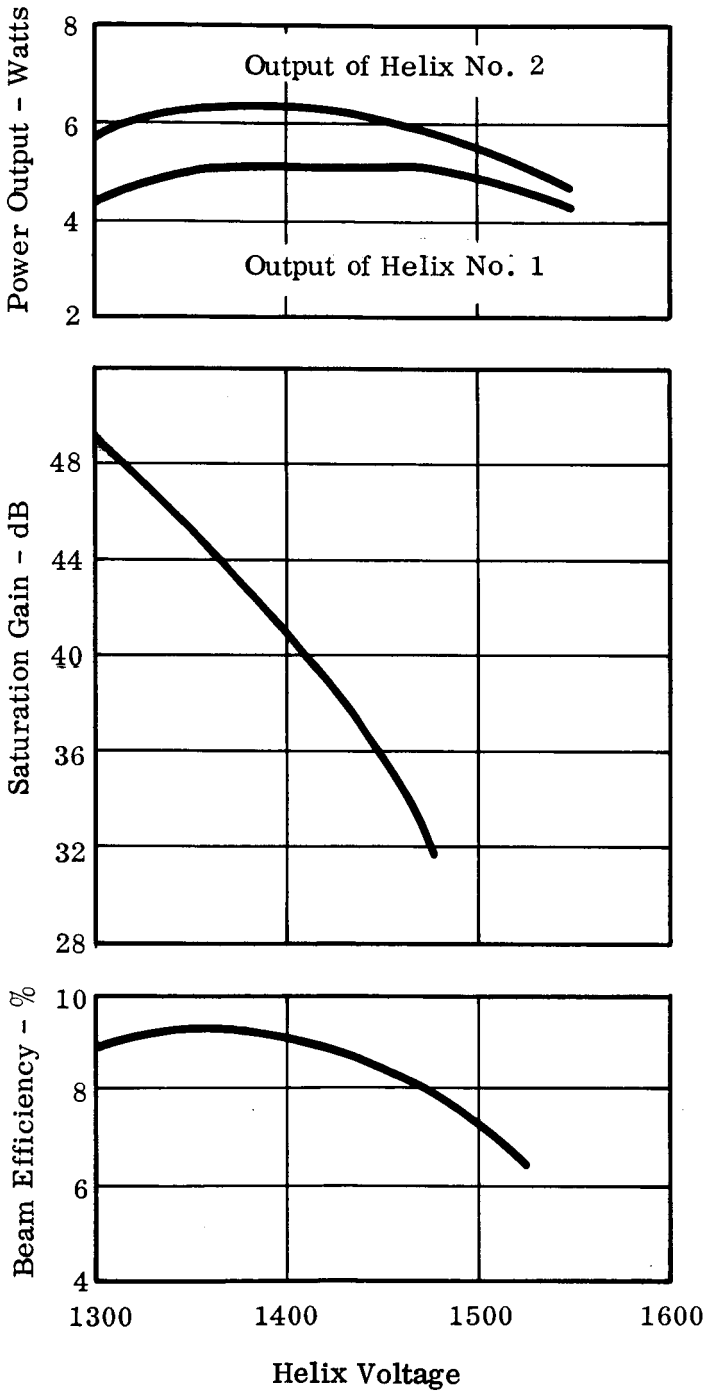

Fig. 22 - Measurements on WJ-274 No. 14 after an organic etching solution had been passed through the helix sections in an attempt to remove the metal deposits. Beam current = 50 mA.

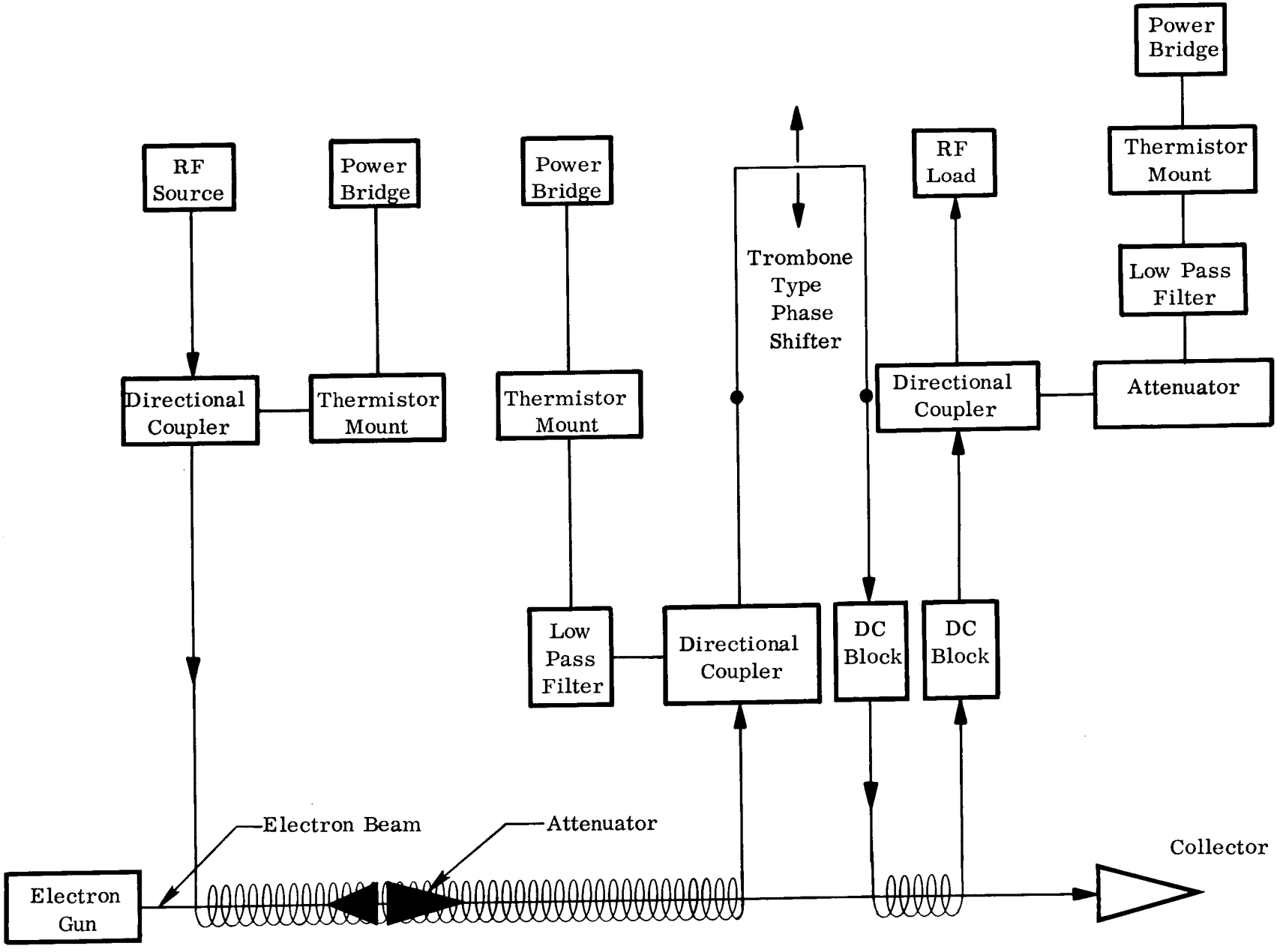

Fig. 23 - Block diagram of test set-up of two-helix tube.

developed a VSWR greater than 4:1. The exact cause was not determined, but could have either been due to alloy bridging two-helix turns or a movement of the impedance wall transducer causing it to touch the helix. In any case, the tube was rendered unusable. The output section was removed and used in tests with organic etching solution prior to reworking tube no. 14 which was described previously.

Discussion of Disadvantages of the Two-Helix Approach

Two-helix tubes were built on this program and also on the 100 watt development program for the Jet Propulsion Laboratory. Both programs met with about equivalent success on this type of tube. The results of the construction and testing of these tubes did not prove or disprove the value of the two-helix tubes as an efficiency enhancement device. But, from the experience gained on these two programs, certain disadvantages of this type of tube can be seen. These are discussed below:

1. Construction Complication

The construction of the two-helix tube is difficult. It took more than twice the effort to construct it compared to a comparable single helix tube. The configuration of the second sever is not ideal. There is almost no room to mount the impedance reducers at the helix to coax transistions and fasten them inside of the tube barrel because of the restricted space. In addition, the body braze becomes very difficult at the second sever. This is due to the fact that there are rigid pole piece and outer conductor assemblies on either side of the second sever. These drain the heat away from the braze joint and require a much longer application of heat to accomplish this braze. Since the helices are already mounted in the body assemblies at this time, it subjects them to excessive temperature and the possibility of evaporation of lossy coating onto the helix support rods. This could ultimately be corrected by redesigning this joint to be closed with a heliarc weld. The body and sever parts would have to be redesigned in this area. The technique of performing the weld would have to be worked out with practice pieces and perhaps special electrodes because the accessibility of the joint is poor because of the window mounts which overlap the joint.

2. Drift Length of the Sever

The second sever occurs in the large signal region of the electron beam interaction. Since there is a practical minimum mechanical distance of two magnet cells from the end of the helix no. 1 to the beginning of helix no. 2, the electron beam must drift in a field free region for this distance. This is not good practice

in the large signal region because appreciable space charge forces exist in the beam at this point. These can cause debunching in the absence of a strong RF electric field on the helix and quite possibly will effect efficiency performance. Even with the same physical length as in the Niclas-Gerchberg two-helix tube, it will be electrically twice as long because of the operating frequency which is slightly more than twice as high. No experiments have been performed to show how critical this drift length is on efficiency performance.

3. Secondary Electron Emission at the Second Sever

This problem confuses the picture of beam transmission. The three current components due to (1) primary electron interception, (2) secondary electron interception and, (3) returned electrons from the depressed collector are indistinguishable. The dissipation due to the secondary electron component is much lower because the electrons are accelerated only across the voltage difference between helices. It is hard to judge how much electron interception can be tolerated under these conditions before damage is done to the helix. It further confuses the meter readings because the helix which emits the secondaries has that current component subtracted from its primary interception component and can in some cases read negative becasue the secondary current is greater than the primary.

4. Impedance Matching of Second Helix

Matching of the short, low-loss, unattenuated second helix to the external transmission line is a difficult task because we have not been able to find a satisfactory way to adequately terminate this short section of helix. Since it cannot be properly terminated, standard reflection coefficient or VSWR measurements made looking into the helix through the external transmission line do not give a simple picture of the discontinuity between the helix and transmission line. In the normal helix with center attenuation, the helix is so well terminated that the discontinuity between the helix and the transmission line represents the only source of reflection. In that case it is simple to adjust the transition for minimum reflection. In the case of the short low-loss section of helix, it is necessary to attempt to terminate the helix with an insertable termination. We were not able to make one with a sufficiently low reflection coefficient of its own and enough attenuation to isolate the discontinuity at the opposite end of the helix. Any matching adjustments cancelled out some of the termination reflection and some of the discontinuity component from the opposite end of the helix as well as the discontinuity between the transmission line and the helix. As a result, the effective reflection coefficient of the transmission

line to helix transition is an unknown. This is a problem at both ends of this short helix section.

5. Ion Trapping

One problem which arises as a direct result of the two-helix operation with the helix No. 2 at a higher potential than Helix No. 1 is the trapping of ions in the Helix No. 1 region. The anode which is at a higher potential than the helix acts as an ion block to keep the ions from draining into the cathode for long life reasons. With the helix No. 2 at a higher potential than Helix No. 1, a potential well is formed. Ions which are created by collisions between electrons of the beam and neutral gas molecules in the Helix No. 1 region, do not have enough energy to climb the potential barriers and build up to form an appreciable ion space charge in this region. They tend to neutralize the electron space charge of the beam thereby shrink the beam diameter and form an ion cloud on the tube axis. The RF performance of the tube changes in the presence of the trapped ions because of the change in the beam diameter. The presence of the ions also will induce ion noise modulation on any signals which the tube is amplifying. The magnitude of this effect has not been measured in this tube, but has been the subject of extensive studies elsewhere and has been shown to result in very real problems.

As of the present writing, no satisfactory means of draining this ion beam in this configuration has been devised. Because of the magnetic containment of the beam, the ions cannot be drained radially through the beam to an electrode placed in the tube at the proper location and potential.

6. Extra Voltage Requirements

A further disadvantage of the two-helix structure is the requirement of an extra voltage for Helix No. 2. This is a complication to the power supply and will in general lead to a slightly lower power supply efficiency because of the added transformer windings, rectifiers and filters required.

This added voltage requirement means that the Helix No. 2 must operate at a voltage difference with respect to the body of the tube. There is always the possibility of voltage breakdown or leakage currents building up with time. This latter might occur due to ion deposition of material on the helix rods during the course of life of the tube. This problem does not exist on a tube in which the helix operates at body potential.

7. External DC Blocks

The requirement for the Helix No. 2 to operate at a potential difference with respect to the body also requires a means for isolating the center conductor of the external transmission line from this helix. This then requires a dc block at both windows capable of withstanding the voltage difference. This must be done in such a way that a very high reliability of performance is assured under the full environmental range of conditions including performance through critical pressure. A failure of this dc block could render the tube inoperative. In addition, one of the blocks must be designed to also apply the voltage to the Helix No. 2 without interfering with the RF properties of the block. Commercial versions of such a device are available for use in laboratory tests. It is bulky and unsuitable for use in space systems. A specific device would have to be developed capable of meeting all the requirements.

Conclusions on the Two-Helix Tubes

The results of the tests were certainly not conclusive since efficiency results were masked by loss problems and also to some extent by focusing. It became clear that the construction of this type of tube would always be considerably more difficult. To build a successful version would require special effort to work out certain constructional problems previously discussed. While these two-helix tubes were being constructed, significant advances in the efficiency performance of single-helix, unipotential helix tubes were being achieved on other programs. In addition, an understanding of the parameters controlling efficiency were beginning to emerge from these studies. It was then decided that the best use of the remaining program effort would be to concentrate on single-helix tubes and to change construction techniques sufficiently to get around the loss problems which appear to be potentially inherent with the current construction. This effort led to the construction of tube nos. 17 and 18 which were described in a previous section.

IV GENERAL CONCLUSION

This report describes a program which explored various designs of the WJ-274 traveling-wave tube with the intent of obtaining an improvement in efficiency. Both single-helix (one-helix potential) and two-helix designs were built and tested.

The two-helix experiments were not successful mainly because of construction difficulties and the resulting helix loss problems. It was determined that the two-helix tubes were always more complicated and difficult to build. If an equivalent performance with a single-helix tube could be obtained, this would certainly be the desirable approach.

By far the best performance was obtained with single-helix tubes using a "positive taper" helix design. The following performance was achieved with the best design developed on this program:

Overall Efficiency	42.2 percent at 2.3 GHz Greater than 41 percent from 2.11 to 2.39 GHz
Saturation power output	25 watts
Saturation Gain	34 dB
Focusing	PPM
Cooling	Conduction

APPENDIX I

APPENDIX I

HELIX DESIGN DETAILS OF TUBE NOS. 10 THROUGH 18

The tube type designation WJ-274 with no dash number indicates experimental tubes and as such the serialization of the tubes has been carried over from the original development program (tube designations WJ-274-1, WJ-274-2, etc. indicate tubes built to meet a specific developmental specification). On the program being reported here, tube nos. 10 through 18 were constructed. The following section gives a brief history and helix design detail of each tube built on the program. The other tube design parameters and construction details are thoroughly described in the final report of the original development program.[1]

WJ-274 No. 10

This tube was constructed to duplicate the electrical design of tube no. 4 of the previous program which gave the best overall performance results. It has a slight modification to the collector nose so that there would be no RF coupling from the end of the helix to the collector. This was done so that the collector could be used as an RF current sampler of the spent electron beam emerging from the helix. It amounted to a simple approach to the current analyzer that was built by Niclas and Gerchberg on the USAECOM High Efficiency Study Program. The collector cooler on this tube was designed so that beam collector element in the tube was completely shielded and connected to a coaxial line. The dc voltage was applied to the collector element by a dc block and dc side arm connection in the coax line. The ac (ie. RF) component of the collector current was carried by the coax line through a low pass filter to a sampling scope. By this means the fundamental component of the beam current could be measured in both phase and amplitude. The fundamental component of the RF helix voltage was coupled from the RF output of the tube by means of a directional coupler and also fed to a sampling scope. By this means, the phase and amplitude of the fundamental RF voltage and beam current were measured as a function of RF input signal level over the range from small signal to beyond saturation.

Measurements of the phase and amplitude of RF voltage and current were measured as a function of a wide range of helix voltages at different beam currents. From these data, the position for the beginning of a positive taper was chosen for tube no. 11.

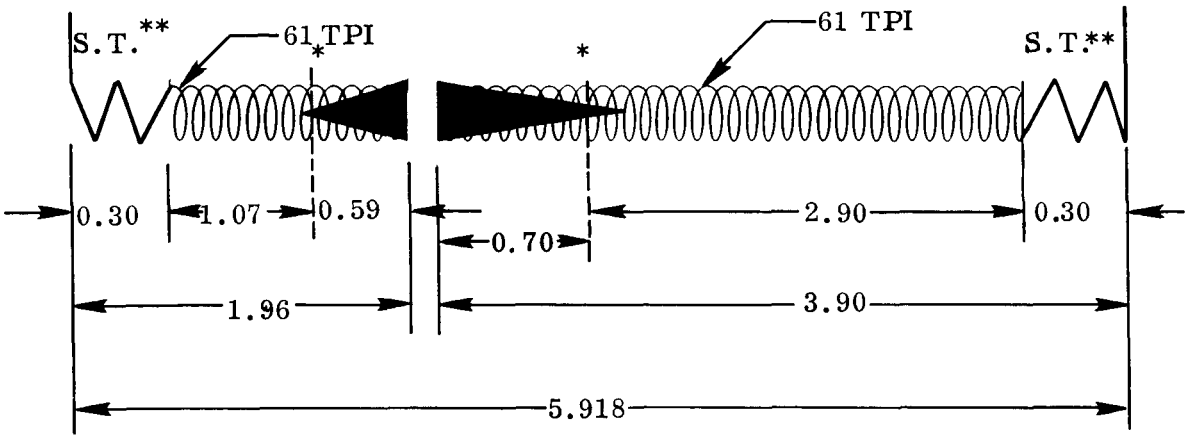

Helix Design of Tube No. 10

* Note that the dashed lines denoting the beginning and end of the attenuator indicate the point where the attenuation has dropped to 1 dB as determined by RF probe measurements of the signal level on the helix and attenuator. This arbitrary point is used as the effective beginning and end of the attenuator.

** S. T. This signifies the Spread Turn Impedance matching section which is five turns of a variable pitch helix. Lengths on all tubes are the same.

WJ-274 No. 11

This tube exhibited an efficiency improvement ratio of 1.32 over tube no. 10 under equivalent operating conditions. But, when both tubes were run under their optimum efficiency conditions (best voltage-current combination), tube no. 10 gave 23.7 percent beam efficiency as compared to 22.3 percent for tube no. 11 at 53 mA. Thus, there appeared to be a decrease in efficiency performance by adding the positive taper to the tube. This was not understood at the time.

In light of the present understanding of the controlling parameters, it is seen that the length of the 61 TPI section of helix was effectively shortened by 0.75 inch by the change that was made. This removed gain from ahead of the positive taper and prevented the large signal section of the tube from being driven sufficiently hard. The taper did have the effect of moving the maximum efficiency point to lower operating voltages.

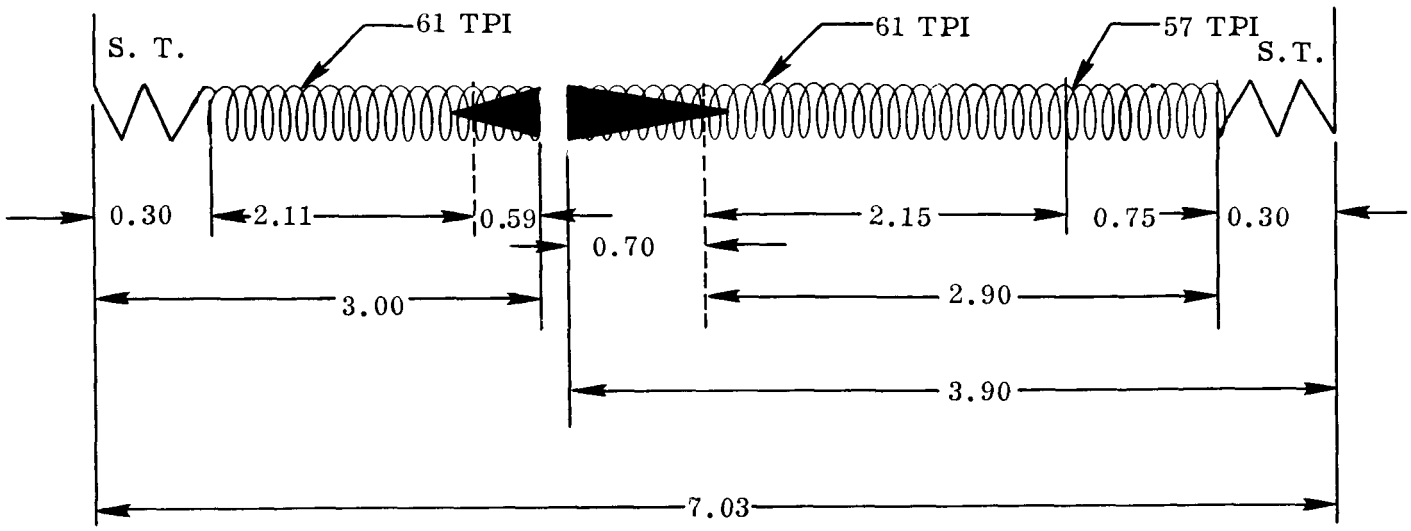

Helix Design of Tube No. 11

WJ-274 No. 12

After noting efficiency performance of tube no. 11 and restudying the phase measurement data of tube no. 10 it was decided that the positive taper had been started in the incorrect place. A decision on a new starting point was made based upon the position along the helix of the maximum phase difference between the voltage and the current and the position of the maximum fundamental component of the RF beam current. Construction was begun on this design and proceeded to the point where helix lock-in took place. Brazing alloy inadvertently came in contact with the helix during this process and permanently shorted turns together. The tube could not be salvaged.

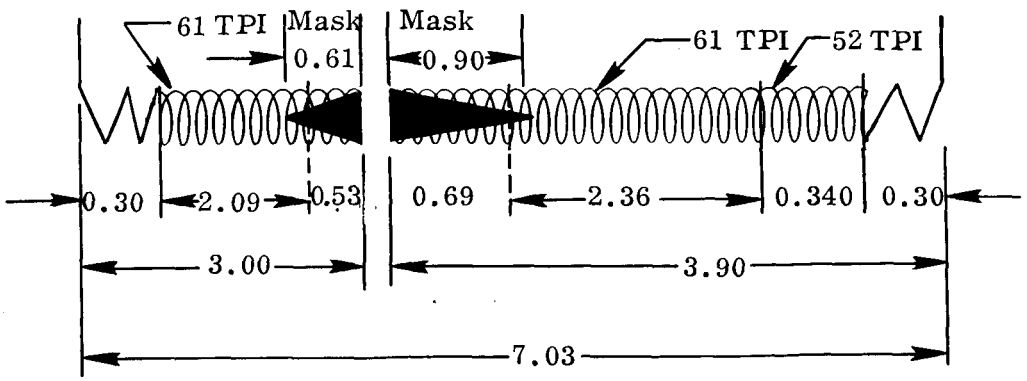

Helix Design of Tube No. 12

with input and output matches. The loss of the helix sections was measured after assembly, after a furnace cycle at brazing temperature and after a vacuum bakeout at 500° C. It was determined that the loss remained at 0.2 dB/wavelength after these operations. This set the ground work for the construction technique used for the following two tubes.

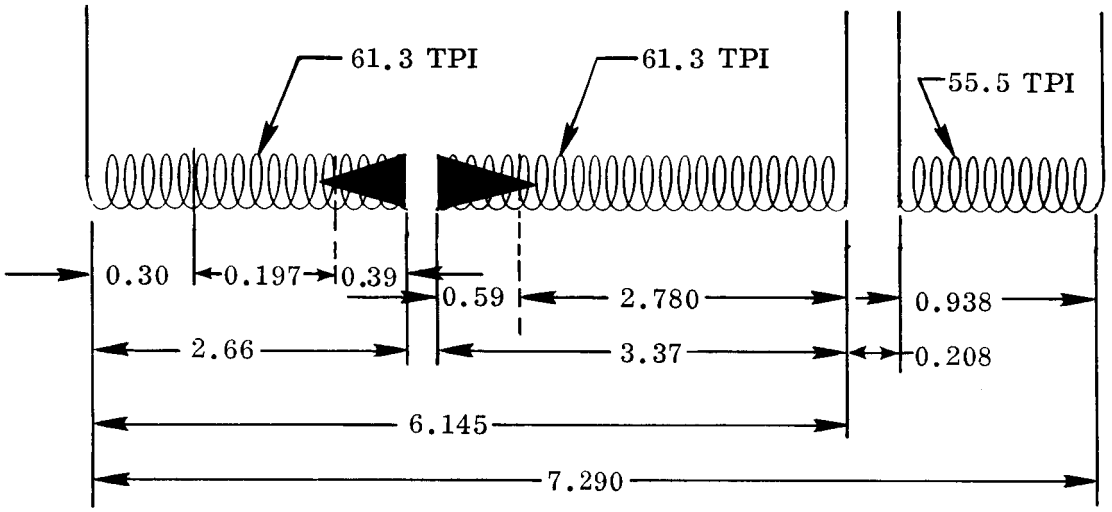

Helix Design of Tube Nos. 15 and 16

WJ-274 No. 17

This tube is patterned after tube no. 13 with a slightly longer positive taper section and a slightly longer section of helix ahead of the positive taper. This latter effect was unprogrammed but occurred because the effective attenuator length turned out to be shorter than planned. One other difference with respect to no. 13 is the 58 TPI input section which was designed to give the tube more than 30 dB gain.

The body-helix construction was changed from the alloy lock-in technique to the triangulated body technique where the body is deformed into a slightly triangular cross-section to allow for helix insertion and then released to spring back and lock the helix in place after release of the deforming forces. The pole pieces are slid onto the body after the helix is inserted and the fit must be very carefully controlled to prevent loose pole pieces. After assembly and processing of the tube it was found that the length of the magnet pole piece assembly was slightly longer than planned so that the magnets fit loosely in the pole pieces. This led to difficulty in focusing and never allowed as good focusing to be achieved as seen in tube no. 13 where the pole pieces are brazed on. As a consequence, the collector depressibility was not as good as no. 13.

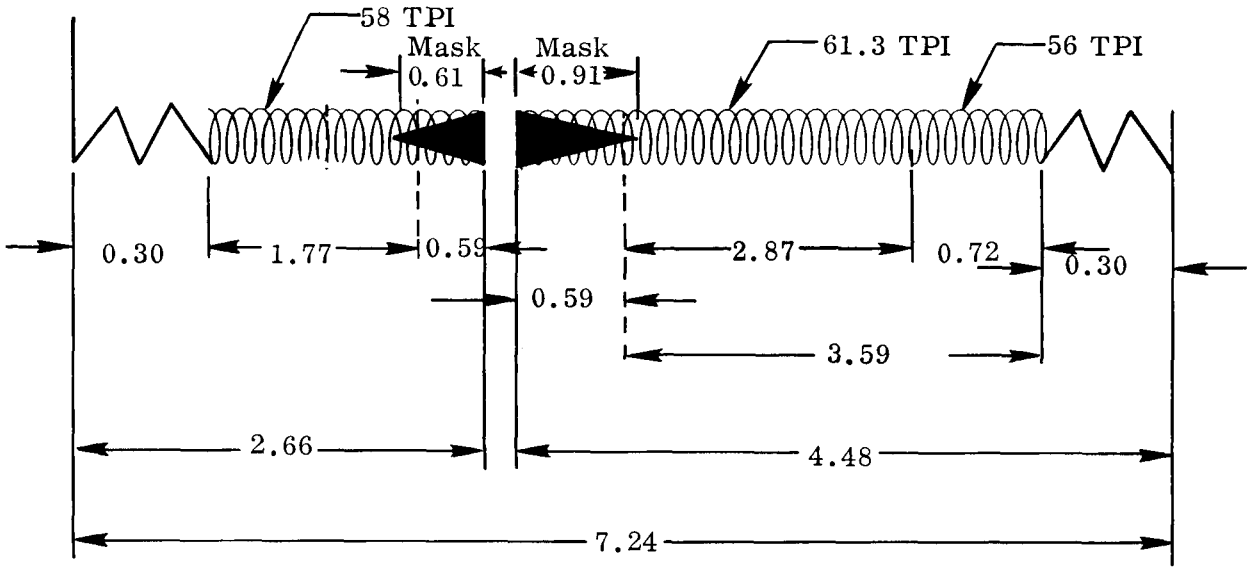

Helix Design of Tube No. 17

WJ-274 No. 18

This tube is very similar in design to tube no. 17 with the exception that the positive taper section is the same length as no. 13 and the length of the helix ahead of the taper was again intended to be the same length as no. 13 but turned out to be slightly longer. The input helix had the same TPI as the output helix. The overall length of nos. 17 and 18 were the same. Both 17 and 18 were built simultaneously, so the design of no. 18 was not based upon the performance of no. 17. This tube also used a triangulated body scheme for locking the helix into the body and had the same magnetic assembly and difficulties as no. 17.

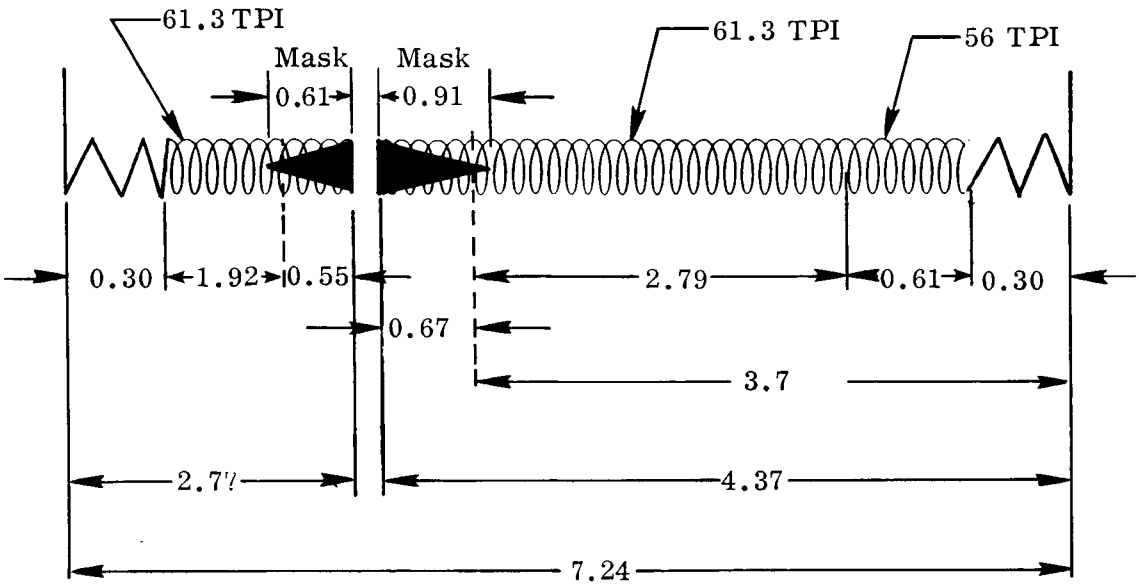

Helix Design for Tube No. 18

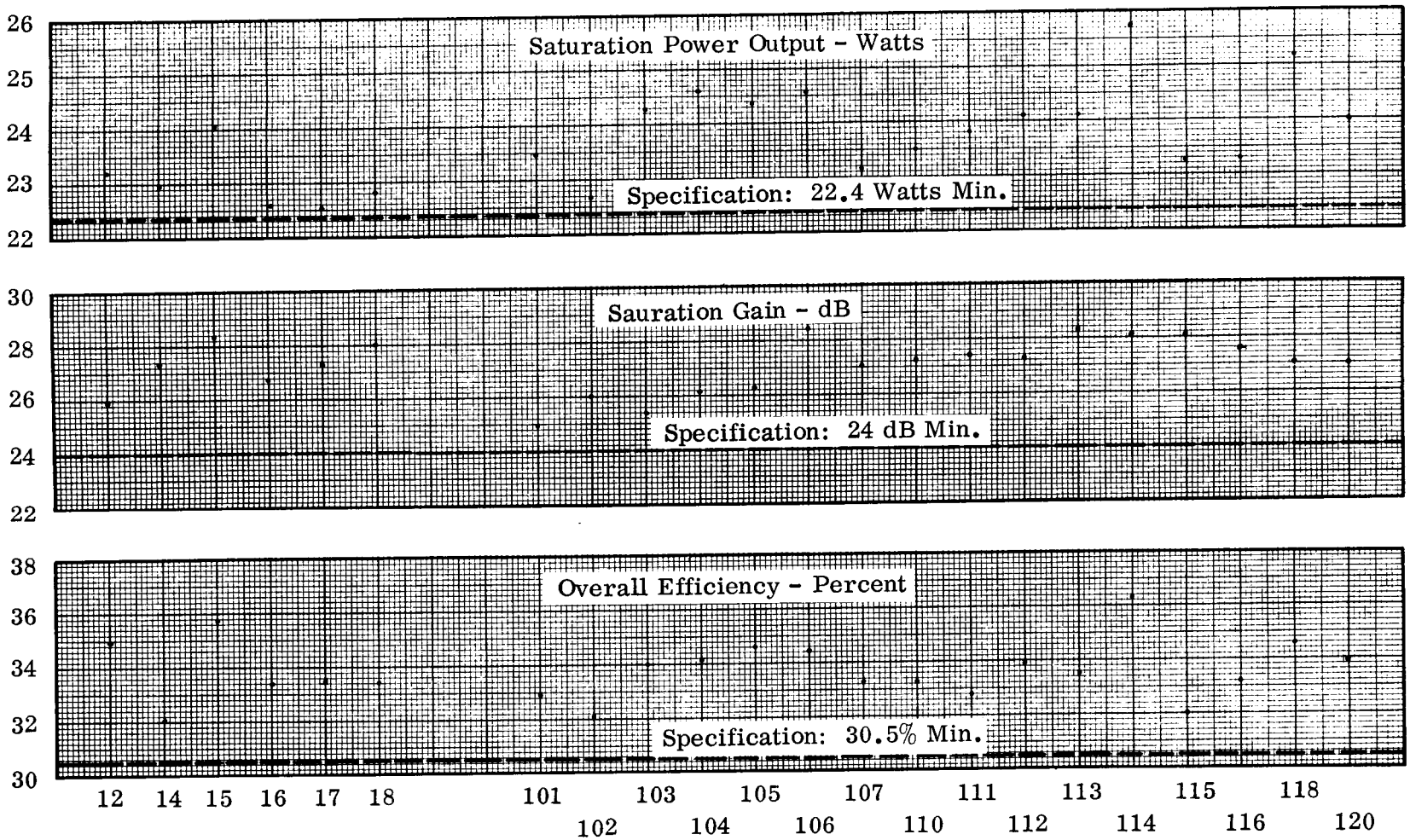

Voltage Range
Anode: 1710 - 1790V
Helix: 1600 - 1660V
Collector: 1140-1200V
Heater: 3.0 - 3.6V

Test Frequency: 2282 MHz

Fig. 23 - WJ-274-1 TWT Performance History.

BIBLIOGRAPHY

1 Roberts, L.A.: The Design and Performance of a High Efficiency Traveling-Wave Tube. Final Report (NAS1-3766), Watkins-Johnson Co., Palo Alto, California.

NASA CR-66522

DISTRIBUTION LIST

NAS1-5923

DEPARTMENT OF DEFENSE	NO. OF COPIES
Defense Documentation Center Attn: DDC-IRS Cameron Station (Bldg. 5) Alexandria, Virginia 22314	1
Office of Assistant Secretary of Defense (Research and Engineering) Attn: Technical Library, Rm 3E1065 Washington, D. C. 20301	1
DEPARTMENT OF THE NAVY	
Naval Ships Systems Command Attn: Code 6454 Department of the Navy Washington, D. C. 20360	1
Director U. S. Naval Research Laboratory Attn: 2027 Washington, D. C. 20390	1
Commanding Officer and Director U. S. Navy Electronics Laboratory Attn: Library San Diego, California 92101	1
DEPARTMENT OF THE AIR FORCE	
Rome Air Development Center (EMTLD) Attn: Documents Library Griffiss Air Force Base New York, 13440	1
Systems Engineering Group (SEPIR) Wright-Patterson Air Force Base Ohio 45433	1
Electronic Systems Division (ESTI) L. G. Hanscom Field Bedford, Massachusetts, 01731	1

DEPARTMENT OF THE ARMY

Chief of Research and Development
Department of the Army
Washington, D. C. 20315 — 1

Commanding General
U. S. Army Material Command
Attention: R & D Directorate
Washington, D. C. 20315 — 1

Redstone Scientific Information Center
Attn: Chief, Document Section
U. S. Army Missile Command
Redstone Arsenal, Alabama 35809 — 1

Commanding Officer
U. S. Army Combat Developments Command
Communications-Electronics Agency
Fort Monmouth, New Jersey 07703 — 1

Harry Diamond Laboratories
Attn: Library
Connecticut Avenue & Van Ness Street
Washington, D. C. 20438 — 1

Commanding Officer
U. S. Army Engineer R & D Laboratories
Attn: Stinfo Branch
Fort Belvoir, Virginia 22060 — 1

U. S. ARMY ELECTRONICS COMMAND

Commanding General
U. S. Army Electronics Command
Fort Monmouth, New Jersey 07703 — 3

Attn: 1 AMSEL-RD-MAT
1 AMSEL-RD-LNA
1 AMSEL-XL-D

OTHER RECIPIENTS

Advisory Group on Electron Devices
346 Broadway, 8th Floor
New York, New York 10013 — 1

NASA Scientific & Technical Info Facility
Attn: Acquisitions Branch (S-AK/DL) 1
P. O. Box 33
College Park, Maryland 20740

Commander
AF Cambridge Research Laboratories 2
Attn: CRZC (1 cy) & CRIM. Mr. Walter Rotman
L. G. Hanscom Field
Bedford, Massachusetts 01731

Director
Advanced Research Projects Agency 1
The Pentagon
Washington, D. C. 20301
Room 2b 285

Commander
AF Avionics Laboratory 1
Wright-Patterson AFB, Ohio 45433
Attn: Mr. Richard D. Alberts, AVIM

Commander
Rome Air Development 1
Griffiss AFB, New York 13442
Attn: Mr. Haralambe Chiosa, EMATE

Director
Naval Research Laboratory
Washington, D. C. 20390
Attn: Mr. Howard O. Lorenzen
Code 4530

Jet Propulsion Laboratory
4800 Oak Grove Drive
Pasadena, California 91103
Attention: Mr. Lloyd Derr 1
Library 1
NASA - Manned Spacecraft Center
2101 Webster Seabrook Road
Houston, Texas 77058
Attention: Mr. Meridth Hamilton 1
Library 1
NASA - Electronics Research Center
575 Technology Square
Cambridge, Massachusetts 02139
Attention: Mr. Carol Veronda 1
Library 1

NASA Flight Research Center
Post Office Box 273
Edwards, California 13523
Attention: Library 1

National Aeronautics and Space Administration
Washington, D. C. 20546
Attention: Mr. O. J. Stanton, Code RET 1
Library, Code USS-10 1

The Boeing Company
Post Office Box 3995
Mail Stop 84-80 MPC
Seattle, Washington 98124
Attention: Mr. N. S. Leach 1
Mr. A. Diestsler 1
Mr. G. H. Hage 1
Mr. I. Hudgins 1

COMSAT Corporation
2100 L. Street, N. W. 1
Washington, D. C. 20037
Attention: Mr. Roberts Strauss

Varian Associates
611 Hansen Way 1
Palo Alto, California 94304
Attention: Dr. Wayne Abraham

Electron Tube Division
Litton Industries 1
960 Industrial Road
San Carlos, California 94070
Attention: Dr. J. F. Hull

Radio Corporation of America
Electronic Components and Devices 1
415 South Fifth Street
Harrison, New Jersey 07029
Attention: Mr. Dick Talpey

NASA - Lewis Research Center
21000 Brookpark Road
Cleveland, Ohio 44135
Attention: Mr. P. W. Kuhns - MS 54-3 1
Library, Mail Stop 3-7 1

NASA - George C. Marshall Space Flight Center
Huntsville, Alabama 35812
Attention: Mr. C. T. Bayer, Code R-ASTR-A 1
Library 1
Mr. Edmund Gleason, Code R-ASTR-IRT 1

Hughes Aircraft Company
Electron Dynamics Division 1
3100 West Lomita Boulevard
Torrance, California 90509
Attention: Mr. K. P. Grabowski

Electronic Communications, Inc.
Post Office Box 12248 1
St. Petersburg, Florida 33733
Attention: Charles V. Gerdes

NASA - Ames Research Center
Moffett Field, California 94035
Attention: John Dimeff, Mail Stop 213-1 1
Library 1

The Ohio State University
1320 Kinnear Road 1
Columbus, Ohio 43212
Attention: Mr. Ross Caldecott
Antenna Laboratory

Air Force Avionics Laboratory
Air Force Systems Command 1
Wright Patterson Air Force Base, Ohio 45433
Attention: Mr. Robert A. Simons, AVWE-2

NASA - Langley Research Center Hampton, Virginia 23365 Attention: Bruce M. Kendall, Mail Stop 473	5
Research Reports Division, Mail Stop 122	5
R. L. Zavasky, Mail Stop 117	1
Library, Mail Stop 185	1
NASA John F. Kennedy Space Center Kennedy Space Center, Florida 32899 Attention: Code ATS-132	1
NASA Western Operations 150 Pico Boulevard Santa Monica, California 90406 Attention: Library	1
NASA Wallops Station Wallops Island, Virginia 23337 Attention: Library	1
NASA Electronics Research Center 575 Technology Square Cambridge, Massachusetts 01239 Attention: Library	1
NASA Michoud Assembly Facility Post Office Box 26078 New Orleans, Louisiana 70126 Attention: Code I-Mich-D	1
NASA Goddard Space Flight Center Greenbelt, Maryland 20771 Attention: Library	1
NASA Scientific and Technical Information Facility Post Office Box 33 College Park, Maryland 20740	30 plus reproducible